



Further lead optimization on Bax activators: Design, synthesis and pharmacological evaluation of 2-fluoro-fluorene derivatives for the treatment of breast cancer



Gang Liu^{a,1}, Hyejin Kim^{b,1}, Pingyuan Wang^a, Doerte R. Fricke^b, Haiying Chen^a,
Tianzhi Wang^c, Qiang Shen^{b,**}, Jia Zhou^{a,c,*}

^a Chemical Biology Program, Department of Pharmacology and Toxicology, University of Texas Medical Branch (UTMB), Galveston, TX, 77555, United States

^b Department of Genetics, Stanley S. Scott Cancer Center, Louisiana State University Health Sciences Center, New Orleans, LA, 70112, United States

^c Sealy Center for Structural Biology and Molecular Biophysics, University of Texas Medical Branch (UTMB), Galveston, TX, 77555, United States

ARTICLE INFO

Article history:

Received 29 January 2021

Received in revised form

2 March 2021

Accepted 27 March 2021

Available online 3 April 2021

Keywords:

Breast cancer therapeutics

Bax activators

Anticancer agents

Drug discovery

Apoptosis

ABSTRACT

To further pursue potent Bax activators with better safety profiles for the treatment of breast cancer, structural optimization was conducted based on lead compound **CYD-4-61** through several strategies, including scaffold hopping on the 2-nitro-fluorene ring, replacement of the nitro group with bioisosteres to avoid potential toxicity, and further optimization on the upper pyridine by exploring diverse alkyl-amine linkers as a tail or replacing the pyridine with bioisosteric heterocycles. F-containing compound **22d** (**GL0388**) exhibited a good balance between the activity and toxicity, displaying submicromolar activities against a variety of cancer cell lines with 5.8–10.7-fold selectivity of decreased activity to MCF-10A human mammary epithelial cell line. Compound **22d** dose-dependently blocked colony formation of breast cancer cells and prevented the migration and invasion of MDA-MB-231 cells. Mechanism of action studies indicate that **22d** activated Bax, rendering its insertion into mitochondrial membrane, thereby leading to cytochrome *c* release from the mitochondria into the cytoplasm, subsequently inducing release of apoptotic biomarkers. Further *in vivo* efficacy studies of **22d** in human breast cancer xenografts arisen from MDA-MB-231 cells demonstrated that this drug candidate significantly suppressed tumor growth, indicating the therapeutic promise of this class of compounds for the treatment of breast cancer as well as the potential for developing F-radiolabeled imaging ligands as anticancer chemical probes.

© 2021 Elsevier Masson SAS. All rights reserved.

1. Introduction

Programmed cell death, a.k.a. apoptosis, is an evolutionarily conserved process that is important in regulating morphogenesis during development and maintaining tissue homeostasis in organs by eliminating unwanted and damaged cells [1]. Inability to respond to apoptotic stimuli leads to a loss of balance between cell division and cell death that accounts for significant reasons of

tumor metastasis and resistance to anticancer drugs [2]. The tumor cells may avoid apoptosis and acquire resistance to apoptotic agents through manipulating several molecular mechanisms. For example, the B-cell lymphoma 2 (Bcl-2) family proteins, which comprise both pro- and antiapoptotic proteins, are the key regulators of mitochondria-mediated apoptosis [3,4]. Bax, a major pro-apoptotic member of the Bcl-2 family proteins, is an indispensable executioner protein that plays a pivotal role in regulating mitochondrial dysfunction and controlling apoptosis in normal and cancer cells [5]. Under normal conditions, Bax largely locates in the cytosol via constant retro-translocation from mitochondria, which avoids unexpected accumulation of toxic Bax levels on the mitochondrial outer membrane (MOM) [6]. Upon stimulation, a conformational change occurs to transform inactive cytosolic monomer into a toxic mitochondrial pore, thus inducing MOM permeabilization and the release of cytochrome *c*, which consequently triggers apoptosis biomarker release and cancer cell apoptosis [7,8].

* Corresponding author. Chemical Biology Program Department of Pharmacology and Toxicology University of Texas Medical Branch, Galveston, TX, 77555, United States.

** Corresponding author. Department of Genetics, Stanley S. Scott Cancer Center, Louisiana State University Health Sciences Center, New Orleans, LA, 70112, United States.

E-mail addresses: qshen@lsuhsc.edu (Q. Shen), jizhou@utmb.edu (J. Zhou).

¹ These authors contribute equally to this work.

Abbreviations			
Bcl-2	B-cell lymphoma 2	HOBt	hydroxybenzotriazole
MOM	mitochondrial outer membrane	EDCI	1-ethyl-3-(3-dimethylaminopropyl)carbodiimide
BC	breast cancer	DMAP	dimethylaminopyridine
TNBC	triple-negative breast cancer	HATU	hexafluorophosphate azabenzotriazole tetramethyl uronium
ER	estrogen receptor	HOAt	1-hydroxy-7-azabenzotriazole
SAR	structure-activity relationship	DIPEA	<i>N,N</i> -diisopropylethylamine
PET	positron emission tomography	TFA	trifluoroacetic acid
HBA	hydrogen bond acceptor	DMF	dimethylformamide
TLC	thin layer chromatography	DAST	diethylaminosulfur trifluoride
UV	ultraviolet	DMSO	dimethyl sulfoxide
HRMS	high-resolution mass spectrometry	EDTA	ethylenediaminetetraacetic acid
HPLC	high-performance liquid chromatography	DDT	dichlorodiphenyltrichloroethane
		ADP	adenosine diphosphate

Breast cancer (BC) is currently the most common cancer and leading cause of cancer-related death in women [9,10]. Despite the fact that typical treatments (e.g. hormone therapy, chemotherapy, targeted therapy and immunotherapy) have achieved a considerable increase in overall response rate and decrease of mortality rate through single or combination therapeutic regimens for BC, the high recurrence risk, unsatisfactory therapeutic outcomes and severe side effects from existent medications create significant drawbacks during current clinical use, which call for innovative therapeutic strategies for BC treatment [11–13]. Recently, accumulating evidence has shown that expression and activation of Bax are strongly correlated with the initiation and progression of BC [14–16]. Specifically, reduced expression of proapoptotic Bax gene and protein was observed in breast cancer patients, in association with a shorter survival in women with metastatic breast adenocarcinoma [14]. On the contrary, enhancing the expression of proapoptotic Bax by chemotherapy treatment induces apoptosis of human BC cell lines [17,18]. Moreover, proof-of-concept studies have provided evidence for direct Bax activation by translocation of Bax to the mitochondria as a treatment strategy in BC and other cancer types [19–22]. Taken together, Bax protein activation to induce cancer cell apoptosis represents a promising strategy to inhibit BC progression with potential advantages to overcome some drawbacks of available anti-BC drugs.

We have recently described our efforts to discover potent Bax activators that target the Ser184 phosphorylation site pocket of Bax as a potential ligand binding site and culminated in the identification of a high throughput hit compound **SMBA1** with 43 nM of binding affinity to Bax protein [23]. Further introducing *O*-alkylamino side chain and replacing carbon atoms with nitrogen of **SMBA1** afforded lead compound **CYD-4-61**, which showed nanomolar level of antiproliferative activities against ER-positive and triple-negative BC cell lines, as well as *in vivo* efficacy of suppressing tumor growth in the MDA-MB-231 xenograft tumor model [24]. However, the indistinct effect against the immortal mammary epithelial cell line (MCF-10A) indicated non-negligible toxicity in the further clinical trials, which prompted us for a continuous structural optimization in pursuit of candidates with good potency and drug-like properties. By analyzing the structure of **CYD-4-61**, the 2-nitro-fluorene fragment appeared to have no direct interactions with the Bax protein in our previous docking analysis [24]. Meanwhile, the nitro group was typically considered as a structural liability despite some existing nitro-containing drugs in clinic, and extensively associated with mutagenicity and genotoxicity [25,26]. Thus, it is imperative to conduct a comprehensive structure-activity relationship (SAR) study on the 2-nitro-fluorene moiety. To pursue novel structures with privileged scaffolds, we

utilized the scaffold hopping method by taking advantage of novel *N*-containing heterocycles as the bioisosteric replacement of fluorene ring. Furthermore, to avoid potential toxicity, we attempted to replace the nitro group with various small substituents, such as methoxy, hydroxyl, fluorine, trifluoromethyl, difluoromethyl, amines, and amides. Herein, we report our effort of structural optimization based on the lead compound **CYD-4-61**, which resulted in the discovery of compound **22d** (**GL0388**) with advanced druglike profiles for further drug development and the potential to develop F-radiolabeled positron emission tomography (PET) imaging ligands for anticancer chemical probes. As depicted in Fig. 1, compound **22d** (**GL0388**) containing 2-fluoro-fluorene ring was obtained with submicromolar antiproliferative activities against BC cell lines and more than 6-fold selectivity of decrease activity towards MCF-10A cells. Moreover, we also employed a brief structural optimization on the upper pyridine ring of **22d** by exploring diverse alkylamine linkers as a tail or replacing the pyridine with bioisosteric heterocycles, to identify potential compounds that better fit the spatial subtleties of the Bax protein and improve the overall drug-like properties.

2. Results and discussion

2.1. Chemistry

The synthetic route for the synthesis of heterocyclic substituted analogues is depicted in Scheme 1. Treatment of 1-bromo-2-iodobenzene with appropriate boronic acids under Suzuki coupling condition [27], followed by palladium-catalyzed formal [4 + 1] annulation generated key intermediates **4** and **6** [28], which were further converted to final compounds **5** and **7**, respectively, through condensation reactions with *tert*-butyl (2-((3-formylpyridin-2-yl)oxy)ethyl)carbamate and subsequent TFA-assisted Boc-deprotection. Compound **5** was afforded as a single enantiomer in 47% yield, while compound **7** was obtained with a 60:40 diastereomeric ratio determined by ¹H NMR analysis in 63% yield [24]. Replacement of the fluorine of 2-fluoro-3-nitropyridine with *tert*-butyl (2-hydroxyethyl) carbamate and then reduction of the nitro group gave intermediate **10**, which was then successfully converted to final compounds **11** and **12** in yields of 57% and 23%, respectively [29]. By condensation of **13** with 2-(1*H*-pyrrol-1-yl)aniline and Boc-deprotection, compound **15** was generated in 33% yield. Reduction of **13** with NaBH₄ followed by bromination in the presence of NBS and PPh₃ provided intermediate **17**. Coupling of **17** with pyrrolo[1,2-*a*]quinoxalin-4(5*H*)-one [30] followed by the Boc-deprotection generated compound **18** in 68% yield.

The analogues with diversified substituents on the fluorene were obtained as a mixture of *Z/E* isomers. As shown in Scheme 2,

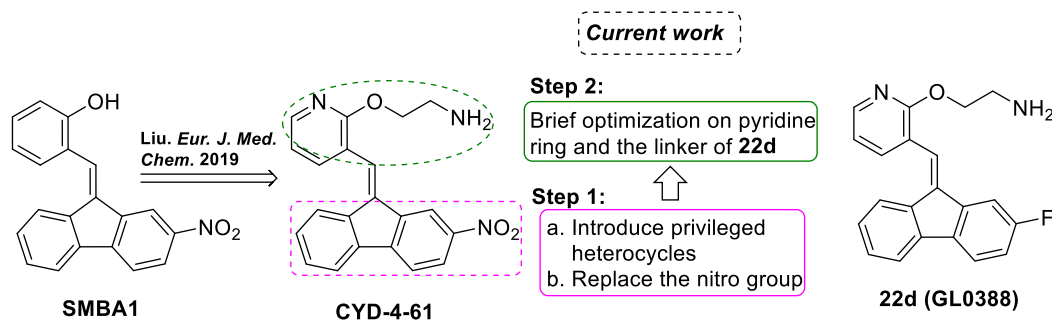


Fig. 1. Structural optimization of lead compound **CYD-4-61** to achieve a new candidate **22d**.

compounds **22a-e** (*dr*, 50:50) were obtained through a Suzuki coupling, [4 + 1] annulation, condensation with *tert*-butyl (2-((3-formylpyridin-2-yl)oxy)ethyl)carbamate, and subsequent deprotection procedure in a similar fashion to that of the preparation of **4** in 23–63% overall yields. By demethylation of **22a** in the presence of BBr_3 , compound **23** (*dr*, 50:50) was afforded in a 71% yield. Treatment of **24** with DAST produced intermediate **25**, which was further converted to the difluoromethyl substituted analogue **26** (*dr*, 50:50) in 72% yield through a similar condensation and deprotection procedure to that for the synthesis of **22a-e**. Compound **28** was obtained by condensation of 2-nitro-9H-fluorene with *tert*-butyl (2-((3-formylpyridin-2-yl)oxy)ethyl)carbamate in 87% yield. Reducing the nitro group of **28**, followed by derivatization with alkyl, acyl, and sulfonyl groups provided compounds **30a-e** (**30a-b**, **30e** (*dr*, 50:50), **30c** (*dr*, 65:35), **30d** (*dr*, 55:45) in 45–76% yields. Finally, intermediate **31** was synthesized by condensation of **27** with 3-methylbut-3-en-1-ol in the presence of $\text{Fe}(\text{acac})_3$, PhSiH_3 , Zn and HCl, which was further converted to compound **32** (*dr*, 60:40) through the similar condensation and de-protection procedure in a yield of 36% [31].

As depicted in Scheme 3, starting material **33** was treated with various hydroxyalkyl carbamates to successfully introduce various alkoxy amine groups to the pyridine ring, followed by the coupling with 2-fluoro-9H-fluorene and Boc-deprotection to afford compounds **35a-d** (*dr*, 50:50) as a pair of diastereomers in 54–77% yields. Intermediate **38** containing pyrazine fragment was prepared through protection of the aldehyde group of **36**, introduction of *tert*-butyl (2-hydroxyethyl)carbamate and the removal of 1,3-dioxolane. Coupling of **38** with 2-fluoro-9H-fluorene and Boc-deprotection afforded compound **39** (*dr*, 50:50) in 50% yield. Analogues containing pyrazolo[1,5-*a*]pyridine fragment were synthesized as depicted in Scheme 4. The key intermediates **41** and **42** were prepared in a total yield of 35% according to a reported literature procedure [32]. The final compounds **44a-b** (*dr*, 50:50) and **46a-b** (*dr*, 50:50) were obtained by coupling of the above mentioned intermediates with 2-fluoro-9H-fluorene leading to compounds **43** and **45**, followed by the introduction of aminoethyl alcohol side chain and Boc-deprotection.

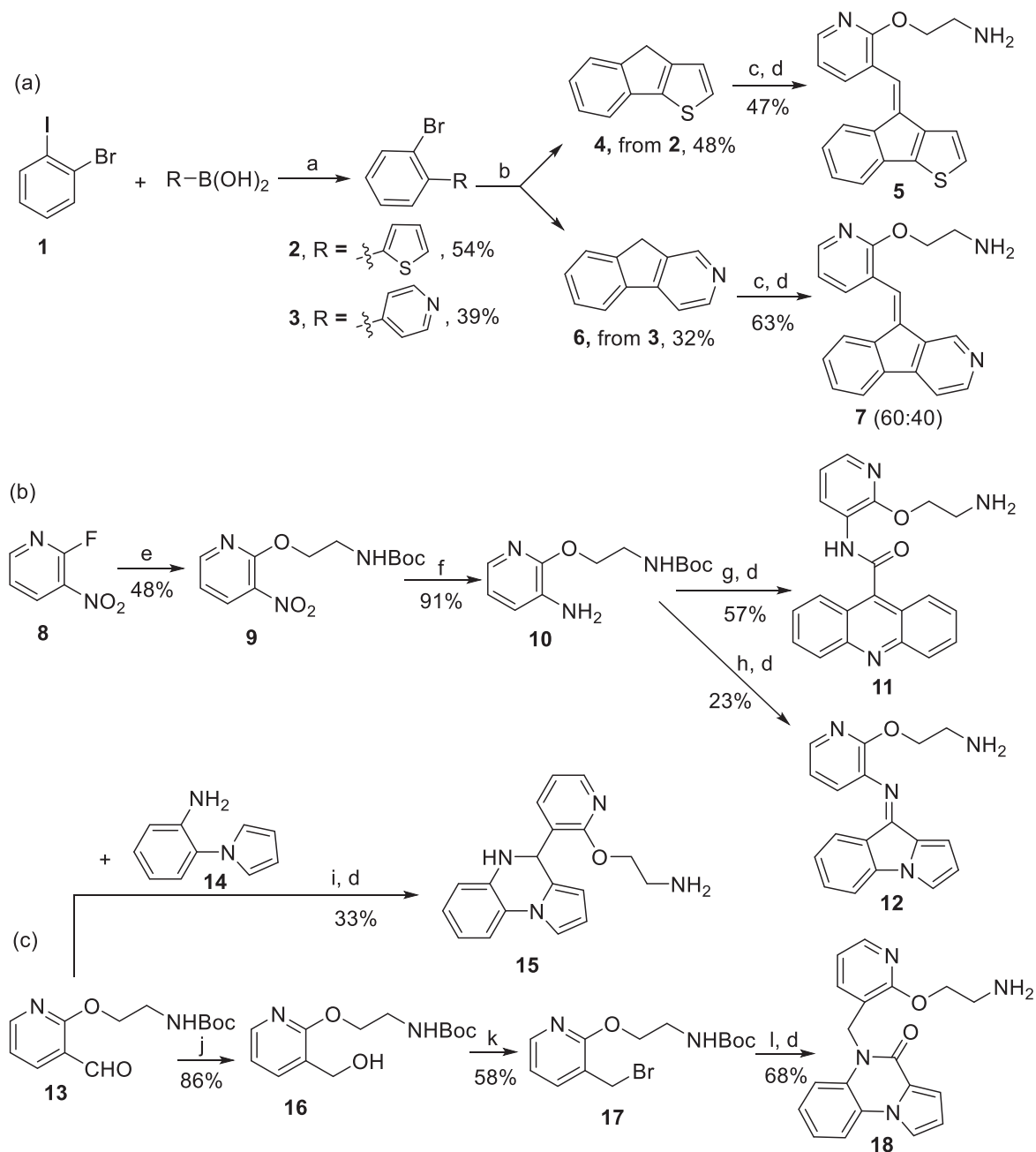
2.2. Biology

2.2.1. Anti-proliferative cellular assay

As previously reported [24], two breast cancer cell lines MDA-MB-231 (triple-negative) and MCF-7 (ER-positive) were chosen for the initial *in vitro* MTT assays to establish the SAR for structural optimization. IC_{50} values were further determined when compounds showed inhibitory rates greater than 50% at the concentration of 10 μM . Similar to what we previously reported, some

compounds with a double bond attached on the fluorene ring were yielded as a mixture of the *E/Z* isomers during the synthesis. Notably, we initially successfully separated the *E/Z* mixture into single isomers by chiral HPLC with a baseline separation; however, the obtained single isomers could dynamically tautomerize to the opposite configurations, eventually leading to an equilibrium mixture of both isomers based on the chiral HPLC analysis. Thus, the pharmacological activities of such compounds were directly tested in an *E/Z* isomer mixture form. We first evaluated the anti-proliferative effects of analogues bearing novel tricyclic rings for the replacement of the 2-nitro-9H-fluorene scaffold of **CYD-4-61**, as summarized in Table 1. Replacement of the fluorene scaffold with 9H-indeno[2,1-*c*]pyridine and 4H-indeno[1,2-*b*]thiophene afforded compounds **5** and **7**, respectively, which showed significantly reduced cytotoxicity compared to **CYD-4-61** but still retained moderate potency against the two cancer cell lines. Further scaffold hopping of the fluorene ring with acridine, 9H-pyrrolo[1,2-*a*]indole, 4,5-dihydropyrrolo[1,2-*a*]quinoxaline and pyrrolo[1,2-*a*]quinoxalin-4(5H)-one led to compounds **11**, **12**, **15**, and **18**, respectively. Interestingly, compounds **11** and **12** were inactive at the testing concentration, while compounds **15** and **18** regained the activities at the low-micromolar range. Among them, compound **15** showed the best activity of this series with IC_{50} values of 2.63 μM and 2.19 μM against MDA-MB-231 and MCF-7 cells, respectively.

Since the analogues obtained in Table 1 only showed moderate to weak potency, our next structural modification strategy focused on replacing the nitro group of fluorene ring with various bio-isosteres to provide compounds with significantly reduced toxicity and less decreased activity of **CYD-4-61**. The SAR study on the nitro group was shown in Table 2. The oxygen of nitro group may provide hydrogen bond acceptor (HBA) to form the direct binding with Bax protein, and thus we first introduced oxygen-containing fragments to mimic the HBA. Specifically, compounds bearing methoxy (compound **22a**) or hydroxyl (compound **23**) group only exhibited moderate potency with IC_{50} values of about 3 μM against MDA-MB-231 and MCF-7 cells. To keep the electron-withdrawing effect of nitro, trifluoromethoxy and amide moieties were introduced to provide compounds **22b** and **22c** with completely abolished activity. Notably, replacement of methoxy of **22a** with fluorine led to compound **22d**, which obviously improved the antiproliferative effect to submicromolar range with IC_{50} values of 0.96 μM and 0.52 μM against MDA-MB-231 and MCF-7 cells, respectively. The significantly increased potency by introducing fluorine atom inspired us to screen other fluorine-containing fragments, such as trifluoromethyl (compound **22e**) and difluoromethyl (compound **26**). Both of them displayed potent anticancer activities, especially difluoromethyl-containing compound **26**, which was only slightly less potent than **22d** with IC_{50} values of 1.27 μM and 1.66 μM

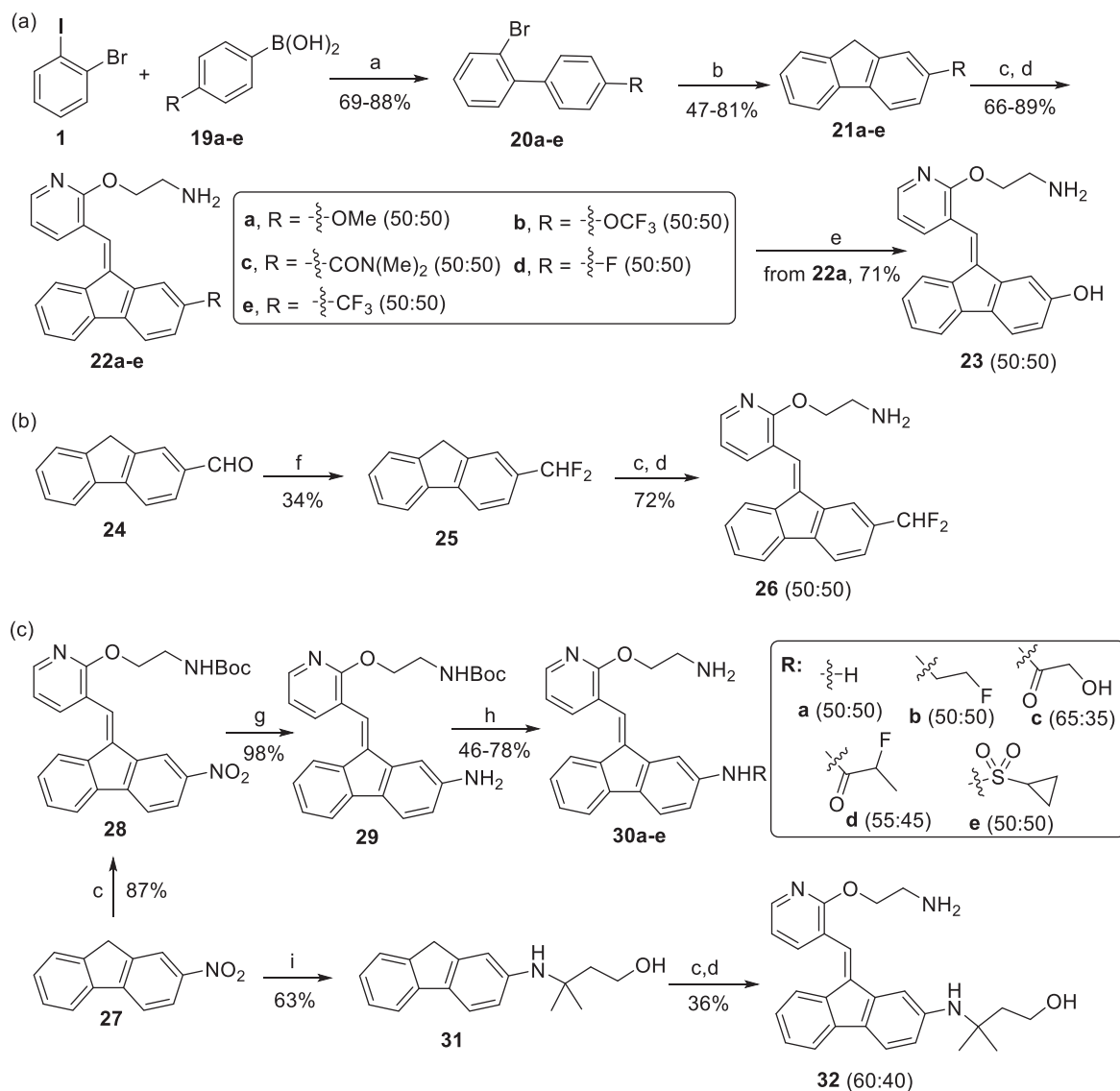


Scheme 1. Synthesis of compounds 5–18. Reagents and conditions: (a) Pd(PPh₃)₄, Na₂CO₃, Toluene/EtOH (2:1), 80 °C, overnight; (b) TMSCHN₂, Pd(PPh₃)₄, K₂CO₃, KOAc, 1,4-dioxane, N₂, 100 °C, overnight; (c) *tert*-butyl (2-((3-formylpyridin-2-yl)oxy)ethyl)carbamate, KF-Al₂O₃, MeOH, 70 °C, overnight; (d) TFA, CH₂Cl₂, RT, 5 h; (e) *tert*-butyl(2-hydroxyethyl)carbamate, Na₂CO₃, DMF, 110 °C, 3 h; (f) Pd/C, H₂, MeOH, RT, overnight; (g) acridine-9-carboxylic acid, EDCI, DMAP, CH₂Cl₂, RT, overnight; (h) 2-(1*H*-pyrrol-1-yl)benzaldehyde, 135 °C, air, 2 h; (i) AcOH, EtOH, 50 °C, 2 h; (j) NaBH₄, EtOH, RT, 4 h; (k) NBS, PPh₃, THF, 0 °C ~ RT, 2 h; (l) pyrrolo[1,2-*a*]quinoxalin-4(5*H*)-one, Cs₂CO₃, MeCN, 60 °C, 6 h.

against MDA-MB-231 and MCF-7 cells, respectively. These results suggest that fluorine atom in the fluorene ring is favorable for retaining the anticancer activities of these compounds. In addition, the nitro group was extensively associated with mutagenicity and genotoxicity [33], which was likely the major reason for the high toxicity of **CYD-4-61**. Thus, reduction and further modification effort was embarked on the nitro group to reduce the potential toxicity. As shown in the right panel of Table 2, the amine compound **30a** was completely inactive. Introduction of alkyl substituents to amine constructing compounds **30b** and **32** restored moderate activities. Notable discrepancies were observed in the

branched amide-containing compounds **30c** and **30d**, among which only compound **30d** retained good potency, whereas compound **30c** with a hydroxyl substituent showed no activity at the tested concentrations. Additionally, the sulfonamide-containing compound **30e** only showed marginal activity.

The SAR study in Table 2 indicates the 2-fluoro-fluorene ring as a privileged scaffold, and hence further structural modification was conducted on the upper pyridyl ring by screening various side chains or replacing the side chain with other novel heterocycles. As shown in Table 3, extending the linker to 3-carbon (**35a**) or shielding one hydrogen of amine with methyl (**35b**) showed 5–10-

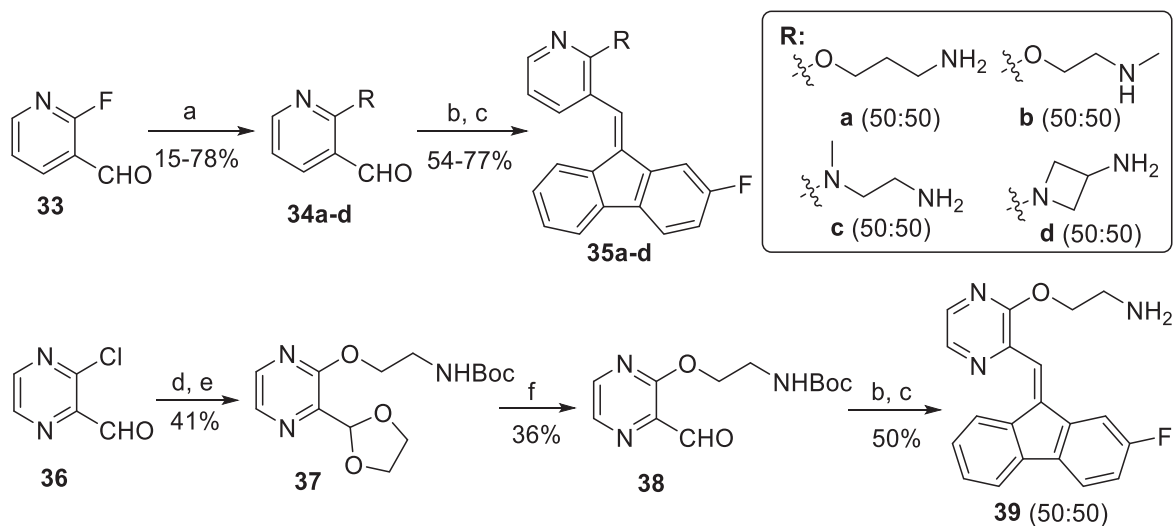


Scheme 2. Synthesis of compounds **22a-e**, **23**, **26**, **30a-e**, **32**. Reagents and conditions: (a) Pd(PPh₃)₄, Na₂CO₃, toluene/EtOH (2:1), 80 °C, overnight; (b) TMSCHN₂, Pd(PPh₃)₄, K₂CO₃, KOAc, 1,4-dioxane, N₂, 100 °C, overnight; (c) *tert*-butyl 2-((3-formylpyridin-2-yl)oxy)ethylcarbamate, KF·Al₂O₃, MeOH, 70 °C, overnight; (d) TFA, CH₂Cl₂, RT, 5 h; (e) BBr₃, CH₂Cl₂, RT, overnight; (f) DAST, CH₂Cl₂, RT, overnight; (g) NH₄Cl, Zn, THF/H₂O, 2 h; (h) for **30a**, TFA, CH₂Cl₂, RT, 5 h; for **30b**, BrCH₂CH₂F, K₂CO₃, KI, DMF, 90 °C, 24 h, then TFA, CH₂Cl₂, RT, 5 h; for **30c** and **30d**, RCOOH, HOBt, EDCI, DMAP, CH₂Cl₂, overnight, then TFA, CH₂Cl₂, RT, 5 h; for **30e**, cyclopropanesulfonyl chloride, DIPEA, CH₂Cl₂, RT, 2 h; then TFA, CH₂Cl₂, RT, 5 h; (i) 3-methylbut-3-en-1-ol, Fe(acac)₃, PhSiH₃, EtOH, 60 °C, 1 h, then Zn, HCl, RT - 60 °C 1 h.

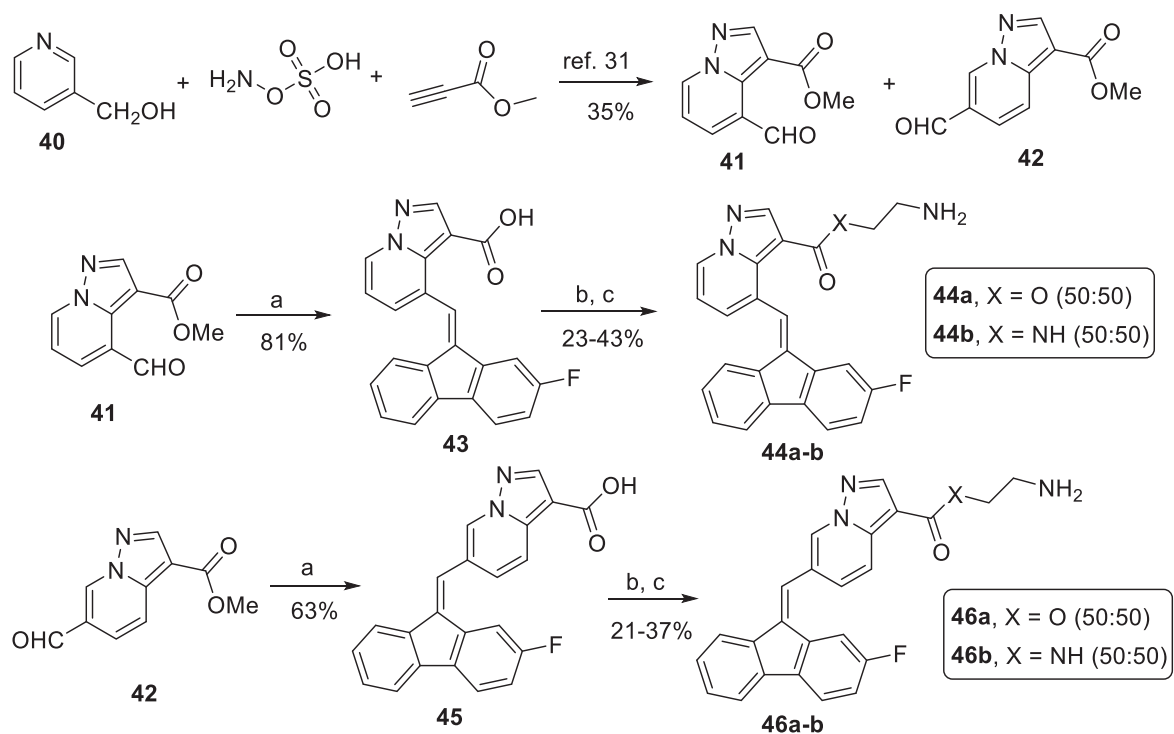
fold reduced activity against MDA-MB-231 and MCF-7 cells compared to **22d**. Replacement of oxygen atom with nitrogen by either *N*-methyl (**35c**) or azetidine (**35d**) also displayed weak activities. These results highlighted the critical contribution of the terminal 2-aminoethan-1-oxygen pharmacophore as the side chain. In addition, bioisosteres of pyridyl ring, such as pyrazinyl was introduced to afford compound **39**, which strikingly decreased the antiproliferative potency compared to that of **22d**. Finally, a pair of pyrazolo[1,5-*a*]pyridine-containing ester and amide isomers were incorporated into the 2-fluoro-fluorene scaffold leading to compounds **44a-b** and **46a-b**, which displayed good potency at a low-micromolar range except the amide analogue **44b** with abolished activities. Compound **46a** was the most potent analogues of this series with IC₅₀ values of 2.04 μM and 1.36 μM against MDA-MB-231 and MCF-7 cells, respectively, despite the slightly more potent compound **22d**.

2.2.2. Compound **22d** (**GL0388**) showed minimal toxicity and best selectivity index (SI) towards human mammary epithelial cell line MCF-10A

As the inhibitory effect of compounds against human mammary epithelial cell line MCF-10A was highly related to *in vivo* toxicity in breast cancer model [24,34,35], several representative compounds (**7**, **22d**, **26**, **46a**) with submicromolar *in vitro* activities were chosen for screening of their antiproliferative effects against MCF-10A cells to evaluate their potential toxicities. The selectivity of compounds against MCF-10A cells compared to MDA-MB-231 and MCF-7 cells was provided as SI (a) and SI (b) respectively, as depicted in Fig. 2 and shown in Table 4. Not surprisingly, the parent compound **CYD-4-61**, which suffered from severe *in vivo* toxicity, only showed SI value of less than 2. Compound **7** bearing 9*H*-indeno[2,1-*c*]pyridine scaffold also showed no obvious selectivity to the MCF-10A cells. Interestingly, compound **22d** with the nitro group



Scheme 3. Synthesis of compounds **35a-d** and **39**. Reagents and conditions: (a) for **34a**, *tert*-butyl (3-hydroxypropyl)carbamate, Na₂CO₃, DMF, 110 °C, 12 h; for **34b**, *tert*-butyl (2-hydroxyethyl)(methyl)carbamate, NaH, THF, 0 °C, 30 min; for **34c**, *tert*-butyl (2-hydroxyethyl)carbamate, K₂CO₃, MeCN, 80 °C, 3 h; for **34d**, *tert*-butyl azetidin-3-ylcarbamate, Na₂CO₃, DMF, 110 °C, 3 h; (b) 2-fluoro-9H-fluorene, KF·Al₂O₃, MeOH, 70 °C, overnight; (c) TFA, CH₂Cl₂, RT, 5 h; (d) ethane-1,2-diol, TsOH, toluene, 110 °C, 5 h; (e) *tert*-butyl (2-hydroxyethyl)carbamate, NaH, THF, 50 °C, overnight; (f) 1 N HCl, MeOH, RT, overnight.



Scheme 4. Synthesis of compounds **44a-b** and **46a-b**. Reagents and conditions: (a) 2-fluoro-9H-fluorene, KF·Al₂O₃, MeOH, 70 °C, 48 h; (b) for **44a**, *tert*-butyl (2-hydroxyethyl)carbamate, EDCI, DMAP, CH₂Cl₂, RT, overnight; for **44b** and **46b**, *tert*-butyl (2-aminoethyl)carbamate, HATU, HOAt, DIPEA, CH₂Cl₂, RT, overnight; for **46a**, *tert*-butyl (2-hydroxyethyl)carbamate, HATU, HOAt, DIPEA, CH₂Cl₂, RT, overnight, then reflux 24 h; (c) TFA, CH₂Cl₂, RT, 5 h.

replacement by fluorine atom significantly increased the SI(a) value to 5.8 and SI(b) to 10.7, respectively, indicating an improved toxicity profile and a potentially enlarged therapeutic window for the *in vivo* efficacy studies compared to **CYD-4-61**. Further replacing the fluorine of **22d** with difluoromethyl leading to compound **26**, declined the selectivity. While compound **46a** containing novel pyrazolo[1,5-*a*]pyridine scaffold also exhibited considerable SI(a)

and SI(b) value, it is less favorable in both activity and SI value compared to **22d**. From the results discussed above, compound **22d** maintained a good balance between the activity against breast cancer cell lines MDA-MB-231 and MCF-7 and the selectivity to the human mammary epithelial cell line MCF-10A, and it was thus selected as a drug candidate for the further mechanistic studies and *in vivo* efficacy evaluation.

Table 1
The antiproliferative effects of analogues **5–18** against MDA-MB-231 and MCF-7 breast cancer cell lines.^{a,b}

Structure	(IC ₅₀ , μM)		Structure	(IC ₅₀ , μM)	
	MDA-MB-231	MCF-7		MDA-MB-231	MCF-7
	5.58 ± 0.36	4.80 ± 0.28		>10	ND
	2.11 ± 0.05	3.10 ± 0.29		2.63 ± 0.74	2.19 ± 0.17
	>10	ND		4.39 ± 0.44	7.88 ± 0.90

^a Software: MasterPlex ReaderFit 2010, MiraiBio, Inc.^b If a specific compound is given a value > 10, it indicates that a specific IC₅₀ cannot be calculated from the data points collected, meaning 'no effect'. The values are the mean ± SD of at least three independent experiments. ND – not determined.**Table 2**
The antiproliferative effects of analogues **22a-e**, **23**, **26**, **30a-e**, and **32** against MDA-MB-231 and MCF-7 breast cancer cell lines.^{a,b}

Entry	R	(IC ₅₀ , μM)		Entry	R	(IC ₅₀ , μM)	
		MDA-MB-231	MCF-7			MDA-MB-231	MCF-7
		3.05 ± 0.32	3.51 ± 0.46	30a		>10	ND
23		2.93 ± 0.21	3.29 ± 0.17	30b		4.79 ± 0.19	4.81 ± 0.24
22b		>10	>10	30c		>10	>10
22c		>10	ND	30d		3.21 ± 0.16	3.69 ± 0.50
22d		0.96 ± 0.2	0.52 ± 0.21	30e		5.29 ± 0.36	5.67 ± 0.67
22e		4.45 ± 0.34	4.85 ± 0.57	32		5.21 ± 0.15	5.04 ± 0.13
26		1.27 ± 0.08	1.66 ± 0.17	–	–	–	–

^a Software: MasterPlex ReaderFit 2010, MiraiBio, Inc.^b If a specific compound is given a value > 10, it indicates that a specific IC₅₀ cannot be calculated from the data points collected, meaning 'no effect'. The values are the mean ± SD of at least three independent experiments. ND – not determined.

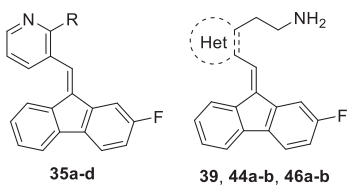
2.2.3. Compound **22d** (**GL0388**) showed broad antiproliferative effects against various cancer cell lines

To further determine whether our Bax activators retained broad

efficacy in various breast cancer cell lines, compound **22d** was evaluated for its growth inhibitory activities against two ER⁺ BC cell line (MCF-7, MDA-MB-361) and three TNBC cell lines (MDA-MB-

Table 3

The antiproliferative effects of analogues **35a-d**, **39**, **44a-b**, and **46a-b** against MDA-MB-231 and MCF-7 breast cancer cell lines.^{a,b}



Entry	R or	(IC ₅₀ , μM)	
		MDA-MB-231	MCF-7
35a		5.31 ± 0.1	5.23 ± 0.14
35b		4.80 ± 0.21	4.33 ± 0.38
35c		6.00 ± 0.77	6.53 ± 0.24
35d		6.21 ± 0.53	5.78 ± 0.52
39		5.33 ± 0.40	4.36 ± 0.57
44a		2.16 ± 0.33	1.95 ± 0.11
44b		>10	ND
46a		2.04 ± 0.35	1.36 ± 0.24
46b		3.04 ± 0.65	2.56 ± 0.30

^a Software: MasterPlex ReaderFit 2010, MiraiBio, Inc.

^b If a specific compound is given a value > 10, it indicates that a specific IC₅₀ cannot be calculated from the data points collected, meaning 'no effect'. The values are the mean ± SD of at least three independent experiments. ND – not determined.

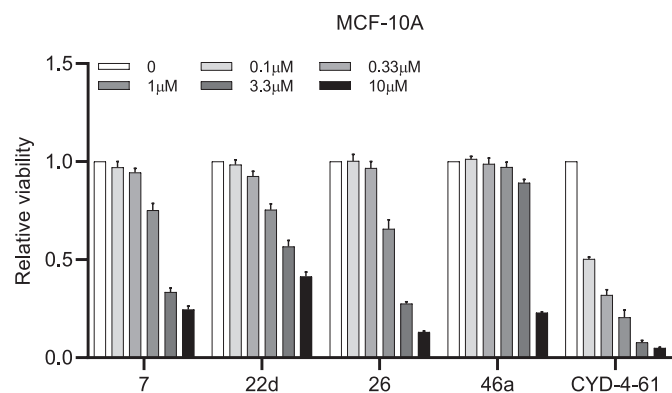


Fig. 2. Growth-inhibitory effects of compounds **CYD-4-61**, **7**, **22d**, **26**, and **46a** against human mammary epithelial cell line MCF-10A. MCF-10A cells were treated with these compounds at indicated concentrations for 72 h. The values are the mean ± SE of at least three independent experiments.

Table 4

The toxicity of representative compounds against human mammary epithelial cell line MCF-10A characterized by selectivity index (SI).^{a,b}

Compounds	(IC ₅₀ , μM)			SI (a)	SI (b)
	MDA-MB-231	MCF-7	MCF-10A		
CYD-4-61	0.07 ± 0.03	0.06 ± 0.03	0.11 ± 0.02	1.6	1.8
7	2.11 ± 0.05	3.10 ± 0.29	2.93 ± 0.42	1.4	0.94
22d	0.96 ± 0.2	0.52 ± 0.21	5.58 ± 1.57	5.8	10.7
26	1.27 ± 0.08	1.66 ± 0.17	1.73 ± 0.16	1.4	1.1
46a	2.04 ± 0.35	1.36 ± 0.24	6.67 ± 0.17	3.3	4.9

^a Software: MasterPlex ReaderFit 2010, MiraiBio, Inc.

^b The values are the mean ± SE of at least three independent experiments. The values are the mean ± SD of at least three independent experiments. SI (a): SI (MCF-10A/MDA-MB-231); SI (b): SI (MCF-10A/MCF-7).

231, MDA-MB-468, BT-549) at the indicated concentrations using MTT assays. As shown in **Table 5**, compound **22d** was found to significantly inhibit the growth of ER⁺ and TNBC cell lines with low micromolar to submicromolar IC₅₀ values. Furthermore, an anti-cancer *in vitro* screening in 60 human tumor cell lines was conducted in a collaboration with the National Cancer Institute Developmental Therapeutics Program. The dose-response curves from five-dose screening (ranging from 0.01 μM to 100 μM) were generated for the determination of three criteria, GI₅₀, TGI, LC₅₀, which represent the drug concentration resulting in 50% of growth inhibition, total Growth Inhibition, and 50% of tumor cells killed, respectively (**supporting information**). The data for representative cancer cells, as depicted in **Table 6**, indicate significant anti-proliferative effects of compound **22d** with GI₅₀ values at the sub-micromolar range level, which further support the pivotal pro-apoptotic role of Bax in a variety of cancer cells as described in previous studies [8,36,37].

2.2.4. Effects of compound **22d** (GL0388) on colony formation and invasion assay in BC cells

Considering the most potent activities against MDA-MB-231 and MCF-7 cell lines, we further test compound **22d** in clonogenic cell survival assay to evaluate its effects on colony formation properties. The colony formation assay performed with **22d** at five doses (0.1 μM, 0.2 μM, 0.3 μM, 0.5 μM, 1 μM), as shown in **Fig. 3a** and **b**, resulted in a significant dose-dependently blocking effect on the clonogenic ability of both BC cell lines. Consistent with the sub-micromolar IC₅₀ value of **22d** from above mentioned cytotoxic studies, more than half of colony formation was blocked at the concentration of 0.5 μM and almost no colony formation was observed at 1 μM. Chemotherapeutic drugs that can simultaneously induce apoptosis and inhibit migration and invasion of cancer cells show promising clinical values [38,39]. The MDA-MB-231 cell line was chosen for evaluating the ability of **22d** in blocking migration and invasion of cancer cells. As exhibited **Fig. 3c** and **d**, the migration and invasion of MDA-MB-231 was dose-dependently inhibited by incubating with **22d** (0.1 μM, 0.5 μM, and 1 μM) for 24 h, showing that compound **22d** inhibits both cancer cell viability and migration and invasion.

2.2.5. Effects of compound **22d** (GL0388) on apoptosis-related biomarkers

Bax insertion in mitochondria and oligomerization in MOM is responsible for mitochondrial apoptosis [8,40]. To test whether **22d** promotes Bax insertion into mitochondrial membranes, MDA-MB-231 cells were treated with increasing concentration of **22d** for 24 h and subsequently the level of Bax protein was analyzed by Western blot. Results from **Fig. 4a** showed that **22d** enhanced Bax insertion into mitochondria in a dose-dependent manner, however less

Table 5
The antiproliferative effects of **22d** against various breast cancer cell lines.^{a,b}

	MDA-MB-231	MCF-7	MDA-MB-468	MDA-MB-361	BT-549
22d	0.96 ± 0.2	0.52 ± 0.21	2.43 ± 0.34	7.13 ± 2.11	3.80 ± 0.31

^a Software: MasterPlex ReaderFit 2010, MiraiBio, Inc.^b The values are the mean ± SE of at least three independent experiments.

potent than **CYD-4-61**. Furthermore, a dose-dependent increase of cytochrome *c* was detected in the cytosolic fraction for MDA-MB-231 cells with **22d** treatment for 24 h (Fig. 4b). To elucidate the potential mechanism related to apoptosis, the expression of several key apoptotic protein markers was determined by Western blot

Table 6
The antiproliferative effects of compounds **22d** (**GL0388**) against a wide variety of human cancer cell lines conducted by National Cancer Institute Developmental Therapeutics Program.

Cell lines		GI ₅₀ (μM)	TGI (μM)	LC ₅₀ (μM)
Leukemia	CCRF-CEM	0.343	3.85	46.7
	HL-60(TB)	0.335	1.18	5.82
	A549/ATCC	0.299	2.12	6.30
Non-Small Cell Lung Cancer	HOP-62	0.483	2.14	7.98
	HCT-116	0.740	2.26	5.79
Colon Cancer	SW-620	0.533	2.06	5.43
	SF-295	0.368	1.62	5.07
CNS Cancer	U251	0.457	1.80	4.82
	LOX IMVI	0.501	1.93	4.75
Melanoma	M14	0.705	2.37	6.72
	OVCAR-3	1.57	2.97	5.62
Ovarian Cancer	NCI/ADR-RES	1.21	2.60	5.61
	786-0	0.575	1.94	4.90
Renal Cancer	ACHN	0.344	1.37	3.78
	PC-3	1.18	2.54	5.46
Prostate Cancer	DU-145	0.400	1.65	4.71

analysis. As shown in Fig. 4c, treatment of MDA-MB-231 cells with **22d** for 48 h significantly led to the upregulation of cleaved PARP-1 and cleaved caspase 3. The above analysis suggests that Bax activation by **22d** results in Bax insertion into mitochondrial membrane, thereby leading to cytochrome *c* release from mitochondria into the cytoplasm, consequently inducing the release of apoptotic biomarkers to trigger the intrinsic apoptotic signaling pathway.

2.2.6. Molecular docking of compound **22d** (**GL0388**) into the Ser184 binding pocket of bax

To illustrate the possible binding mode of compound **22d** to Bax protein, we performed molecular docking studies using the published NMR solution structures of Bax (PDB ID: 1F16) and

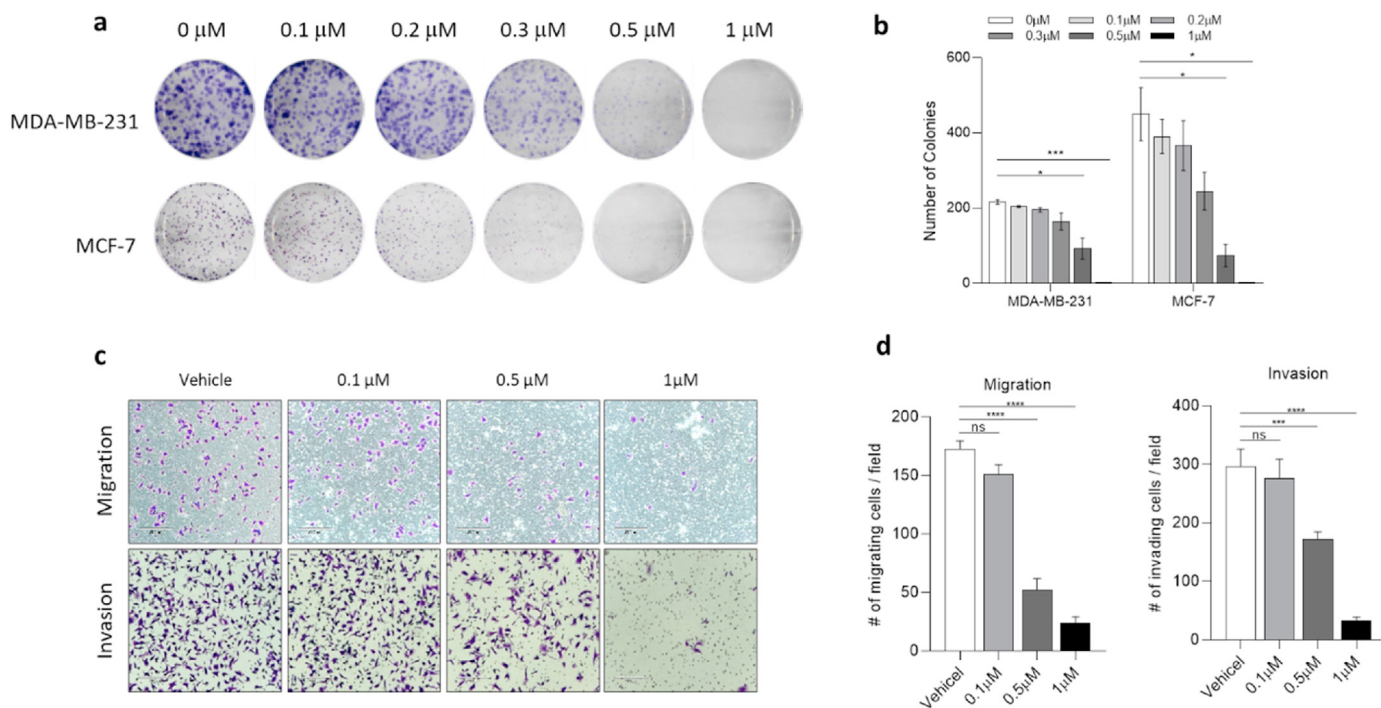


Fig. 3. Effects of compound **22d** on colony formation and invasion of breast cancer cells. (a) Representative photograph of colony formation, **22d** was used in a single treatment to treat MDA-MB-231 and MCF-7 cancer cells for one week at 0, 0.1 μM, 0.2 μM, 0.3 μM, 0.5 μM and 1 μM concentrations. (b) Quantification of colony-formation assay results showing decrease of colony numbers compared to DMSO vehicle treatment. (c) MDA-MB-231 cells were incubated with **22d** (0.1 μM, 0.5 μM, and 1 μM) for 24 h, then the cells were seeded in chambers and incubated for 8 h to assess migration and 16 h to assess invasion. (d) Quantification of migration and invasion assay results of MDA-MB-231 cells. **P < 0.01; ***P < 0.001; ****P < 0.0001; ns, not significant; Student *t*-test. Three independent experiments were performed.

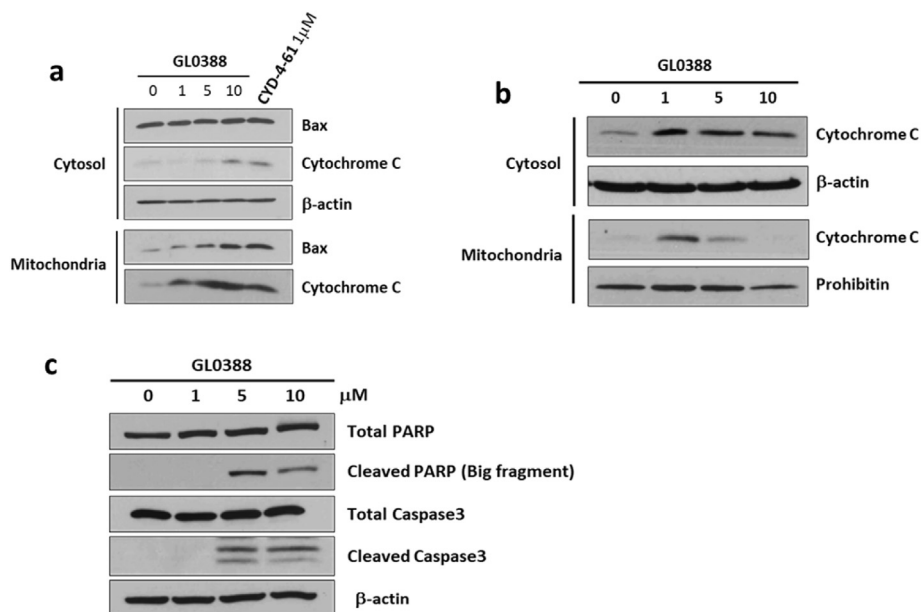


Fig. 4. Bax activation-mediated intrinsic apoptosis in BC cells with compound **22d** (**GL0388**). (a) MDA-MB-231 cells were treated with **22d** at 1 μM, 5 μM and 10 μM as indicated. **CYD-4-61** at 1 μM was used as positive control. The expression of Bax in mitochondria was determined by Western blot analysis. (b) Western blot analysis of cytochrome c in cytosolic and mitochondrial fractions after treatment with **22d** (1 μM, 5 μM, and 10 μM) for 24 h. (c) Western blot analysis of apoptotic biomarkers induced by **22d** at various concentrations (48 h).

Schrödinger Small Molecule Drug Discovery Suite (Schrödinger Release 2020-4, Schrödinger, LLC, New York, NY, 2019). The docking results suggest that compound **22d** can be docked into the Ser184 phosphorylation site binding pocket in the C terminus of Bax protein (Fig. 5a-b), in a similar conformation to the predicted binding mode of lead compound **CYD-4-61** from our previous docking study [24]. The *O*-alkylamino side chain forms a hydrogen bond with the residue Asp98, and the nitrogen atom of the pyridine ring forms a hydrogen bond with the residue Arg109, which is consistent with our previous analysis. The docked pose revealed that the 2-fluoro-fluorene ring of **22d** forms an additional F-H bond interaction directly with Ser184, in comparison with the binding mode of **CYD-4-61**.

2.2.7. *In vivo* anticancer efficacy of compound **22d** (**GL0388**)

The effects of **22d** in suppression of tumor growth *in vivo* was evaluated by using intraperitoneal injection (I.P.) and intratumoral injection (I.T.) administration in an aggressive triple-negative

breast cancer xenograft model with MDA-MB-231 cells. As shown in Fig. 6a, compound **22d** was found to dose-dependently suppress the growth of MDA-MB-231 tumors following the I.P. administration. Compared to the vehicle control, **22d** significantly inhibited tumor growth at a dose of 15 mg/kg every other day. I.T. administration for 10 consecutive days, with an inhibition rate of 55%, comparable to the I.P. efficacy at the dose of daily 20 mg/kg. Tumor shrinking was clearly visible in mice of both I.P. and I.T. groups compared to vehicle control (Fig. 6b). Slight body weight loss was observed in the I.P. administration group. While **22d** by I.T. administration did not cause animal deaths or obvious body weight loss (Fig. 6c), tumor-specific drug delivery strategies (e.g., nanoparticles and bioorthogonal chemistry approach [41]) to further reduce the potential toxicity and enlarge the therapeutic window would be helpful and will be pursued in our future research plan. Importantly, apoptosis-related biomarkers were also detected in tumor tissues from both I.P. and I.T. administration groups. As shown in Fig. 6d, increased level of Bax in the I.T. group and cleaved

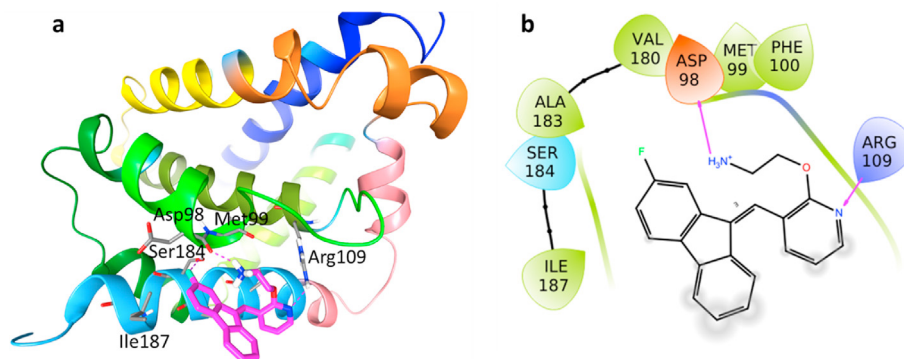


Fig. 5. (a) **22d** (magenta) docking into Ser184 site binding pocket of Bax protein (PDB ID: 1F16) in ribbon representation. Binding site residues are shown in sticks. Hydrogen bonds including F-H bond interaction directly formed between the fluorine of 2-fluoro-fluorene ring with Ser184 are shown as dotted purple lines. (b) Interaction diagram of the predicted binding site. The F-H bond interaction was identified but not shown in the interaction diagram.

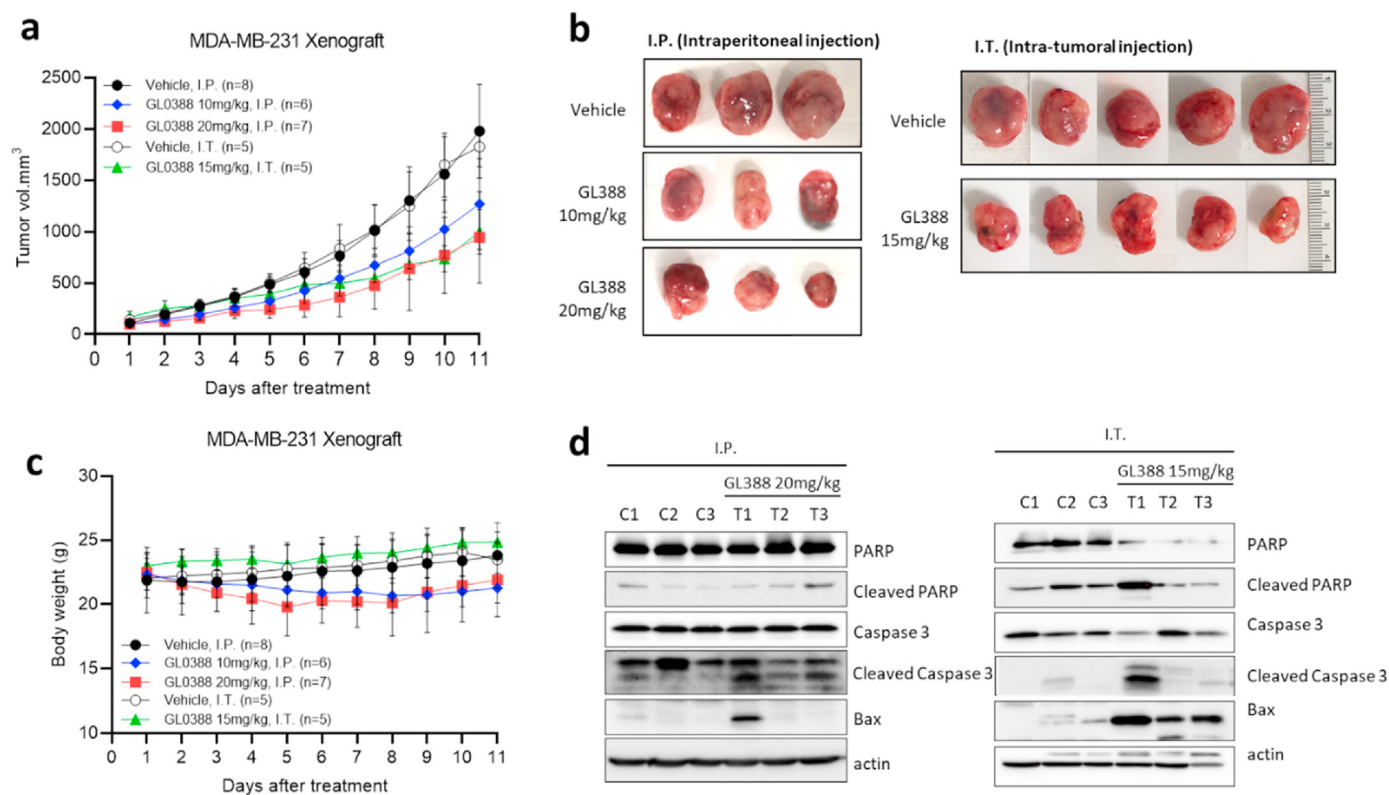


Fig. 6. *In vivo* efficacy of compound **22d** in inhibiting the growth of MDA-MB-231 xenograft tumors in mice (I.P.). (a) Nude mice with MDA-MB-231 xenografts were treated with **22d** at 10 and 20 mg/kg intraperitoneal administration and 15 mg/kg intra-tumoral (I.T.) administration for 10 days. Data is presented as the mean \pm SD of tumor volume at each time point. (b) Tumor images of representative mice. (c) Mean body weight of control-treated and **22d**-treated animals. (d) Representative Western blots for Bax and apoptosis markers from tumors; C, control; T, tumor.

PARP and caspase 3 in both groups were observed from Western blot analysis, further supporting the Bax activation with Bax inserting into mitochondrial membranes to induce the release of apoptotic biomarkers that trigger the intrinsic apoptotic signaling pathway.

3. Conclusion

As a continuous study for pursuing potent Bax activators with better safety profiles for the treatment of breast cancer, we conducted a systematic structural optimization campaign based on the 2-nitro-fluorene moiety of lead compound **CYD-4-61** through several strategies, including scaffold hopping by taking advantage of novel *N*-containing heterocycles as the bioisosteric replacement of fluorene ring, and replacement of the nitro group with various small substituents to avoid potential toxicity. In addition, we also employed a meaningful optimization on the upper pyridine by exploring diverse alkylamine linkers and side chains as a tail or replacing the pyridine with a variety of bioisosteric heterocycles. The synthesized analogues were screened for their antiproliferative effects against both triple-negative BC (e.g., MDA-MB-231) and ER-positive BC (e.g., MCF-7) cell lines. Among them, compound **22d** (**GL0388**), a fluorinated analog, not only showed submicromolar activity against breast cancer cells and a panel of other tumor cells, but also exhibited 5.8–10.7-fold selectivity to the human mammary epithelial cell line MCF-10A, indicating a good balance between the anticancer activity and cytotoxicity selectivity. Compound **22d** was further observed to dose-dependently block the clonogenic ability of both BC cells, as well as prevent the migration and invasion of MDA-MB-231 cells. Mechanism of action

studies suggest that Bax activation by **22d** results in inserting into mitochondrial membranes, thereby leading to cytochrome *c* release from mitochondria to the cytoplasm, consequently inducing the release of apoptotic biomarkers and promoting cancer cell apoptosis. Furthermore, compound **22d** at 20 mg/kg by I.P. administration and 15 mg/kg by I.T. administration showed significant tumor growth inhibition efficacy in MDA-MB-231 tumor xenograft model, as well as increased expression of apoptosis-related biomarkers from tumor tissue samples. Collectively, compound **22d** may serve as a good lead compound for further extensive structural optimization and tumor-specific drug delivery strategies towards future therapeutic development. In addition, this potent fluorine-containing drug candidate may have the potential to develop F-radiolabeled positron emission tomography (PET) imaging ligands for anticancer chemical probes.

4. Experimental protocols

4.1. Chemistry

All reactions were performed in glassware containing a stir bar and the commercially available starting materials and all the commercially available chemical reagents and solvents were reagent grade and used without further purification. The reactions were performed under an air atmosphere unless otherwise stated. Preparative column chromatography was performed using silica gel 60 and a particle size of 0.063–0.200 mm (70–230 mesh, flash). Analytical TLC was carried out employing silica gel 60 F254 plates (Merck, Darmstadt, Germany). Visualization of the developed chromatograms was performed with detection by UV (254 nm). ^1H

and ^{13}C spectra were recorded on a Bruker-600 (^1H , 300 MHz; ^{13}C , 75 MHz; ^{19}F , 300 MHz) spectrometer with CDCl_3 , $\text{CDCl}_3 + \text{CD}_3\text{OD}$ or $\text{DMSO}-d_6$ as the solvent and TMS as an internal reference. Chemical shifts down-field from TMS were expressed in parts per million, and J values were given in hertz.

4.1.1. 2-((3-((4*H*-Indeno[1,2-*b*]thiophen-4-ylidene)methyl)pyridin-2-yl)oxy)ethan-1-amine (5)

Thiophen-2-ylboronic acid (256 mg, 2.0 mmol) and $\text{Pd}(\text{PPh}_3)_4$ (116 mg, 0.1 mmol) were added to an oven-dried Schlenk flask. After degassed with N_2 , 1-bromo-2-iodobenzene (622 mg, 2.2 mmol), toluene (8 mL), ethanol (4 mL) and 1 M Na_2CO_3 aqueous solution (4 mL) were added and the reaction mixture was stirred at 80 °C overnight. After cooled to room temperature, 10 mL of Et_2O was added and the organic layer was then washed with saturated brine (10 mL) and dried over anhydrous Na_2SO_4 . The solvent was evaporated *in vacuo* and the resulting residue was purified by silica gel chromatography to give compound **2** as a colorless oil. Yield 255 mg, 54%. Compound **2** (172 mg, 1.0 mmol), $\text{Pd}(\text{PPh}_3)_4$ (57 mg, 0.05 mol), K_2CO_3 (138 mg, 1.0 mmol) and KOAc (98 mg, 1.0 mmol) were mixed in 10 mL of dioxane. After degassed with N_2 , trimethylsilyl diazomethane (2 N in hexane, 0.6 mL, 1.2 mmol) was added via syringe. The mixture was stirred at 100 °C overnight and then filtered through celite. The solvents were evaporated *in vacuo* and the residue was purified by silica gel chromatography to give compound **4** as a pale solid. Yield 82 mg, 48%. To a solution of compound **4** (35 mg, 0.2 mmol) and *tert*-butyl 2-((3-formylpyridin-2-yl)oxy)ethylcarbamate (53 mg, 0.2 mmol) in 10 mL of methanol was added $\text{KF}\cdot\text{Al}_2\text{O}_3$ (39 mg, 0.24 mmol). The reaction mixture was stirred at 70 °C overnight, and then evaporated *in vacuo*. The residue was purified by silica gel column chromatography (ethyl acetate/ CH_2Cl_2 , 1:4) to give an intermediate, which was dissolved in CH_2Cl_2 (5 mL) and TFA (228 mg, 2.0 mmol) was slowly added. The reaction was stirred at rt overnight and then treated with saturated NaHCO_3 (5 mL). The mixture was extracted with CH_2Cl_2 (3 × 10 mL), dried over Na_2SO_4 , filtered, concentrated and purified by silica gel column chromatography ($\text{CH}_2\text{Cl}_2/\text{MeOH}$) to give compound **5** as a pale yellow foam. Yield 30 mg, 47% (two steps). ^1H NMR (300 MHz, CDCl_3) δ 8.19 (dd, $J = 5.1, 1.8$ Hz, 1H), 7.97 (dd, $J = 7.2, 1.8$ Hz, 1H), 7.77–7.74 (m, 1H), 7.46–7.38 (m, 2H), 7.36–7.21 (m, 2H), 7.13 (d, $J = 5.1$ Hz, 1H), 7.03–6.95 (m, 2H), 4.45 (t, $J = 5.4$ Hz, 2H), 3.11 (t, $J = 5.4$ Hz, 2H), 1.78 (s, 2H). ^{13}C NMR (75 MHz, CDCl_3) δ 161.37, 146.54, 145.94, 141.39, 141.24, 139.48, 135.86, 134.13, 128.28, 126.60, 125.41, 122.26, 120.60, 120.04, 119.70, 118.61, 116.54, 68.46, 41.37. HRMS (ESI) calcd for $\text{C}_{19}\text{H}_{17}\text{N}_2\text{OS}$, 321.1062 $[\text{M} + \text{H}]^+$; found, 321.1051.

4.1.2. 9*H*-Indeno[2,1-*c*]pyridine (6)

The synthesis of compound **6** was conducted by following a procedure similar to that of compound **4**. The title compound was obtained as a colorless oil. Yield 112 mg, 32%. ^1H NMR (300 MHz, CDCl_3) δ 8.79 (s, 1H), 8.61 (d, $J = 5.1$ Hz, 1H), 7.88–7.81 (m, 1H), 7.67–7.58 (m, 2H), 7.45–7.40 (m, 2H), 3.93 (s, 2H).

4.1.3. (*E/Z*)-2-((3-((9*H*-Indeno[2,1-*c*]pyridin-9-ylidene)methyl)pyridin-2-yl)oxy)ethan-1-amine (7)

The synthesis of compound **7** was conducted by following a procedure similar to that of compound **5**. The title compound was obtained as a white foam. Yield 21 mg, 63%. ^1H NMR (300 MHz, CDCl_3) δ 9.08 (s, 0.38H), 8.80 (s, 0.62H), 8.59 (d, $J = 5.1$ Hz, 0.38H), 8.53 (d, $J = 5.1$ Hz, 0.62H), 8.25–8.20 (m, 1H), 7.94–7.86 (m, 1.62H), 7.81–7.77 (m, 1H), 7.67 (d, $J = 3.6$ Hz, 1H), 7.62–7.56 (m, 1.38H), 7.52–7.44 (m, 1H), 7.39 (td, $J = 7.6, 1.2$ Hz, 0.62H), 7.24 (td, $J = 7.6, 1.2$ Hz, 0.38H), 7.02–6.97 (m, 1H), 4.47–4.44 (m, 2H), 3.07 (t, $J = 5.4$ Hz, 2H), 2.03 (s, 2H). ^{13}C NMR (75 MHz, CDCl_3) δ 161.16,

149.04, 148.80, 147.87, 147.51, 147.46, 145.18, 142.46, 139.71, 139.53, 139.40, 138.85, 136.94, 136.68, 135.40, 134.10, 131.80, 129.39, 129.04, 128.97, 128.62, 124.41, 123.54, 123.49, 121.40, 121.0, 121.01, 119.36, 119.13, 116.85, 116.62, 114.65, 114.28, 68.44, 68.33, 41.27, 41.18. HRMS (ESI) calcd for $\text{C}_{20}\text{H}_{18}\text{N}_3\text{O}$, 316.1450 $[\text{M} + \text{H}]^+$; found, 316.1440.

4.1.4. *tert*-Butyl 2-((3-nitropyridin-2-yl)oxy)ethylcarbamate (9)

To a solution of 2-fluoro-3-nitropyridine (284 mg, 2.0 mmol) and *tert*-butyl(2-hydroxyethyl)carbamate (645 mg, 4.0 mmol) in DMF (5 mL) was added Na_2CO_3 (424 mg, 4.0 mmol). The reaction mixture was stirred at 110 °C for 3 h, and then water (50 mL) was added. The mixture was extracted with EtOAc (3 × 15 mL), washed with water (3 × 10 mL), dried over Na_2SO_4 , filtered, concentrated *in vacuo* and purified by silica gel column chromatography (hexane/ethyl acetate) to give compound **9** as a white solid. Yield 271 mg, 48%. ^1H NMR (300 MHz, CDCl_3) δ 8.39 (dd, $J = 4.8, 1.8$ Hz, 1H), 8.30 (dd, $J = 7.8, 1.8$ Hz, 1H), 7.07 (dd, $J = 7.8, 4.8$ Hz, 1H), 5.07 (s, 1H), 4.56 (t, $J = 5.4$ Hz, 2H), 3.61 (q, $J = 5.4$ Hz, 2H), 1.46 (s, 9H).

4.1.5. *N*-(2-(2-Aminoethoxy)pyridin-3-yl)acridine-9-carboxamide (11)

To a solution of compound **9** (566 mg, 2.0 mmol) in MeOH (10 mL) was slowly added Pd/C (283 mg). The reaction was stirred under H_2 atmosphere at rt overnight. After the starting material completely consumed, the reaction was filtered and concentrated to provide compound **10** as a colorless oil, which was used directly in the next step without further purification.

To a solution of acridine-9-carboxylic acid (45 mg, 0.2 mmol) in CH_2Cl_2 (2 mL) was added EDCI (78 mg, 0.4 mmol), DMAP (5 mg, 0.04 mmol) and compound **10** (76 mg, 0.3 mmol). The reaction was stirred at rt overnight and then diluted with water (10 mL). The mixture was extracted with CH_2Cl_2 (3 × 5 mL), dried over Na_2SO_4 , filtered, concentrated and purified by silica gel column chromatography (hexane/ethyl acetate) to provide the intermediate.

To a solution of the intermediate (55 mg, 0.12 mmol) in CH_2Cl_2 (3 mL) was slowly added TFA (272 mg, 2.4 mmol). The reaction was stirred at rt overnight and then treated with saturated NaHCO_3 (5 mL). The mixture was extracted with CH_2Cl_2 (3 × 10 mL), dried over Na_2SO_4 , filtered, concentrated and purified by silica gel column chromatography ($\text{CH}_2\text{Cl}_2/\text{MeOH}$) to give compound **11** as a white foam. Yield 41 mg, 57% (two steps). ^1H NMR (300 MHz, CDCl_3) δ 8.92 (dd, $J = 7.8, 1.8$ Hz, 1H), 8.22 (d, $J = 9.0$ Hz, 2H), 8.14 (d, $J = 8.7$ Hz, 2H), 7.94 (dd, $J = 5.0, 1.7$ Hz, 1H), 7.84–7.75 (m, 2H), 7.62–7.52 (m, 2H), 7.05 (dd, $J = 7.8, 5.0$ Hz, 1H), 4.33 (t, $J = 4.9$ Hz, 2H), 2.95 (s, 2H), 2.72 (s, 2H). ^{13}C NMR (75 MHz, $\text{CDCl}_3 + \text{MeOD}$) δ 166.41, 153.66, 148.52, 141.50, 141.21, 130.62, 129.29, 129.13, 126.83, 125.37, 122.44, 117.34, 66.88, 40.48. HRMS (ESI) calcd for $\text{C}_{21}\text{H}_{19}\text{N}_4\text{O}_2$, 359.1518 $[\text{M} + \text{H}]^+$; found, 359.1494.

4.1.6. (*E*)-2-((3-((9*H*-Pyrrolo[1,2-*a*]indol-9-ylidene)amino)pyridin-2-yl)oxy)ethan-1-amine (12)

A mixture of 2-(1*H*-pyrrol-1-yl)benzaldehyde (51 mg, 0.3 mmol) and compound **11** (0.19 g, 2.0 mmol) was heated at 135 °C for 2 h. The resulting mixture was purified by silica gel column chromatography ($\text{CH}_2\text{Cl}_2/\text{EtOAc}$) to give the intermediate as a yellow foam. To a solution of the intermediate (41 mg, 0.1 mmol) in CH_2Cl_2 (3 mL) was slowly added TFA (228 mg, 2.0 mmol). The reaction was stirred at rt overnight and then treated with saturated NaHCO_3 (5 mL). The mixture was extracted with CH_2Cl_2 (3 × 10 mL), dried over Na_2SO_4 , filtered, concentrated and purified by silica gel column chromatography ($\text{CH}_2\text{Cl}_2/\text{MeOH}$) to give compound **12** as a yellow foam. Yield 21 mg, 23%. ^1H NMR (300 MHz, CDCl_3) δ 8.01 (dd, $J = 5.0, 1.8$ Hz, 1H), 7.94–7.86 (m, 1H), 7.44 (td, $J = 7.7, 1.3$ Hz, 1H), 7.32 (dd, $J = 7.5, 1.8$ Hz, 1H), 7.26–7.15 (m, 2H), 7.03 (dd, $J = 2.6,$

0.9 Hz, 1H), 6.96 (dd, $J = 7.5, 5.0$ Hz, 1H), 6.15 (dd, $J = 3.7, 2.7$ Hz, 1H), 5.70 (dd, $J = 3.7, 0.9$ Hz, 1H), 4.35 (t, $J = 5.2$ Hz, 2H), 2.95 (t, $J = 5.2$ Hz, 2H), 1.57 (s, 2H). ^{13}C NMR (75 MHz, CDCl_3) δ 155.44, 154.31, 142.29, 141.99, 135.71, 132.07, 131.57, 128.78, 128.24, 124.90, 123.99, 117.16, 116.16, 114.88, 112.61, 110.03, 68.30, 41.29. HRMS (ESI) calcd for $\text{C}_{18}\text{H}_{17}\text{N}_4\text{O}$, 305.1402 $[\text{M} + \text{H}]^+$; found, 305.1394.

4.1.7. 2-((3-(Pyrrolo[1,2-*a*]quinoxalin-4-yl)pyridin-2-yl)oxy)ethan-1-amine (**15**)

To a solution of 2-(1*H*-pyrrol-1-yl)aniline (158 mg, 1.0 mmol) and 2-(2-aminoethoxy)nicotinaldehyde (266 mg, 1.0 mmol) in EtOH (5 mL) was added 5 drops of AcOH. The reaction mixture was stirred at 50 °C for 2 h, and then evaporated under vacuum and purified by silica gel column chromatography ($\text{CH}_2\text{Cl}_2/\text{EtOAc}$) to give the intermediate as a pale yellow solid. The intermediate was dissolved in CH_2Cl_2 (5 mL), and TFA (1.14 g, 10 mmol) was slowly added. The reaction was stirred at rt overnight and then treated with saturated NaHCO_3 (5 mL). The mixture was extracted with CH_2Cl_2 (3×10 mL), dried over Na_2SO_4 , filtered, concentrated and purified by silica gel column chromatography ($\text{CH}_2\text{Cl}_2/\text{MeOH}$) to give compound **15** as a pale yellow foam. Yield 101 mg, 33% (two steps). ^1H NMR (300 MHz, CDCl_3) δ 7.99 (dd, $J = 5.1, 1.8$ Hz, 1H), 7.32 (dd, $J = 7.8, 1.5$ Hz, 1H), 7.24 (dd, $J = 3.0, 1.5$ Hz, 1H), 7.09 (dd, $J = 7.2, 1.8$ Hz, 1H), 6.89 (td, $J = 7.5, 1.5$ Hz, 1H), 6.81–6.67 (m, 3H), 6.34 (t, $J = 3.0$ Hz, 1H), 5.94–5.92 (m, 2H), 4.53–4.40 (m, 2H), 3.17–3.12 (m, 2H), 2.12 (s, 2H). ^{13}C NMR (75 MHz, CDCl_3) δ 160.53, 145.79, 136.66, 135.22, 126.46, 125.21, 125.11, 124.70, 118.99, 117.15, 115.69, 114.52, 114.31, 110.23, 105.80, 67.79, 49.35, 41.23. HRMS (ESI) calcd for $\text{C}_{18}\text{H}_{19}\text{N}_4\text{O}$, 307.1559 $[\text{M} + \text{H}]^+$; found, 307.1549.

4.1.8. tert-Butyl 2-((3-(bromomethyl)pyridin-2-yl)oxy)ethyl carbamate (**17**)

To a solution of compound **13** (532 mg, 2.0 mmol) in EtOH (10 mL) was slowly added NaBH_4 (152 mg, 4.0 mmol). The reaction was stirred at rt for 4 h and then treated with saturated NH_4Cl (5 mL). The mixture was extracted with CH_2Cl_2 (3×10 mL), dried over Na_2SO_4 , filtered, concentrated and purified by silica gel column chromatography ($\text{CH}_2\text{Cl}_2/\text{EtOAc}$) to give compound **16** in 86% yield as a colorless oil, which was used directly in next step without further purification.

To a solution of compound **16** (54 mg, 0.2 mmol) in THF (5 mL) at 0 °C was added NBS (89 mg, 0.5 mmol) and PPh_3 (131 mg, 0.5 mmol). The reaction was stirred at rt for 2 h and then evaporated under vacuum and purified by silica gel column chromatography (hexane/ CH_2Cl_2) to give compound **17** as a colorless oil. Yield 38 mg, 58%. ^1H NMR (300 MHz, CDCl_3) δ 8.11 (dd, $J = 5.0, 1.9$ Hz, 1H), 7.62 (dd, $J = 7.3, 1.9$ Hz, 1H), 6.89 (dd, $J = 7.3, 5.0$ Hz, 1H), 5.14 (s, 1H), 4.59–4.39 (m, 4H), 3.58 (q, $J = 5.4$ Hz, 2H), 1.46 (s, 9H).

4.1.9. 5-((2-(2-Aminoethoxy)pyridin-3-yl)methyl)pyrrolo[1,2-*a*]quinoxalin-4(5*H*)-one (**18**)

To a solution of pyrrolo[1,2-*a*]quinoxalin-4(5*H*)-one (55 mg, 0.3 mmol) in MeCN (3 mL) was added compound **17** (100 mg, 0.3 mmol) and Cs_2CO_3 (117 mg, 0.36 mmol). The reaction was stirred at 70 °C for 6 h, and then concentrated and purified by silica gel column chromatography ($\text{CH}_2\text{Cl}_2/\text{Ethyl acetate}$) to give the intermediate as a white foam. The intermediate was dissolved in CH_2Cl_2 (5 mL) and TFA (342 mg, 3.0 mmol) was slowly added. The reaction was stirred at rt overnight and then treated with saturated NaHCO_3 (5 mL). The mixture was extracted with CH_2Cl_2 (3×10 mL), dried over Na_2SO_4 , filtered, concentrated and purified by silica gel column chromatography ($\text{CH}_2\text{Cl}_2/\text{MeOH}$) to give compound **18** as a white foam. Yield 68 mg, 68% (two steps). ^1H NMR (300 MHz, CDCl_3) δ 8.03 (dd, $J = 5.1, 1.8$ Hz, 1H), 7.71–7.67 (m, 2H), 7.32–7.13 (m, 5H), 6.77–6.70 (m, 2H), 5.47 (s, 2H), 4.50 (t, $J = 5.3$ Hz,

2H), 3.18 (t, $J = 5.3$ Hz, 2H), 2.26 (s, 2H). ^{13}C NMR (75 MHz, CDCl_3) δ 160.71, 155.78, 145.52, 136.11, 129.14, 125.67, 124.09, 123.14, 122.91, 118.67, 117.14, 116.39, 114.65, 113.46, 113.27, 68.15, 41.37, 39.71. HRMS (ESI) calcd for $\text{C}_{19}\text{H}_{19}\text{N}_4\text{O}_2$, 335.1508 $[\text{M} + \text{H}]^+$; found, 335.1500.

4.1.10. (*E/Z*)-2-((3-((2-methoxy-9*H*-fluoren-9-ylidene)methyl)pyridin-2-yl)oxy)ethan-1-amine (**22a**)

The synthesis of compound **22a** was conducted by following a procedure similar to that of compound **5**. The title compound was obtained as a yellow solid. Yield 58 mg, 72%. ^1H NMR (300 MHz, CDCl_3) δ 8.22 (dd, $J = 5.0, 1.9$ Hz, 1H), 7.98–7.92 (m, 1H), 7.77 (dt, $J = 7.4, 1.0$ Hz, 0.5H), 7.63–7.59 (m, 2H), 7.51 (d, $J = 8.6$ Hz, 1H), 7.47 (dt, $J = 7.8, 0.9$ Hz, 0.5H), 7.39–7.25 (m, 2H), 7.09 (d, $J = 2.4$ Hz, 0.5H), 7.05–6.94 (m, 2H), 6.89 (dd, $J = 8.3, 2.4$ Hz, 0.5H), 4.47–4.43 (m, 2H), 3.93 (s, 1.5H), 3.68 (s, 1.5H), 3.10–3.04 (m, 2H), 1.62 (s, 2H). ^{13}C NMR (75 MHz, CDCl_3) δ 161.28, 161.23, 159.66, 158.93, 147.03, 146.91, 141.46, 141.01, 139.54, 139.43, 139.30, 139.08, 137.97, 137.46, 136.32, 134.57, 132.49, 128.80, 128.45, 125.98, 125.60, 123.99, 121.33, 121.17, 120.48, 120.40, 119.73, 119.67, 119.08, 118.83, 116.59, 116.45, 114.73, 114.51, 109.84, 106.18, 68.52, 55.67, 55.31, 41.36. HRMS (ESI) calcd for $\text{C}_{22}\text{H}_{21}\text{N}_2\text{O}_2$, 345.1603 $[\text{M} + \text{H}]^+$; found, 345.1596.

4.1.11. (*E/Z*)-2-((3-((2-(Trifluoromethoxy)-9*H*-fluoren-9-ylidene)methyl)pyridin-2-yl)oxy)ethan-1-amine (**22b**)

The synthesis of compound **22b** was conducted by following a procedure similar to that of compound **5**. The title compound was obtained as a yellow foam. Yield 31 mg, 81%. ^1H NMR (300 MHz, CDCl_3) δ 8.26–8.22 (m, 1H), 7.93–7.89 (m, 1H), 7.84–7.81 (m, 0.5H), 7.70–7.62 (m, 3H), 7.55–7.52 (m, 1H), 7.42–7.31 (m, 2H), 7.24 (ddd, $J = 8.3, 2.2, 1.1$ Hz, 0.5H), 7.18 (ddd, $J = 8.3, 2.2, 1.0$ Hz, 0.5H), 7.12 (td, $J = 7.6, 1.2$ Hz, 0.5H), 6.98 (ddd, $J = 7.0, 5.0, 1.7$ Hz, 1H), 4.45 (t, $J = 5.4$ Hz, 2H), 3.08–3.04 (m, 2H), 1.69 (s, 2H). ^{13}C NMR (75 MHz, CDCl_3) δ 161.20, 148.67 (q, $J = 1.7$ Hz), 147.91 (q, $J = 1.7$ Hz), 147.49, 147.31, 140.93, 139.82, 139.46, 139.34, 137.93, 137.76, 137.67, 136.65, 136.47, 136.43, 128.96, 128.60, 127.35, 126.98, 124.15, 122.95, 122.79, 121.35, 121.09, 120.63, 120.56 (q, $J = 266$ Hz), 120.49 (q, $J = 255$ Hz), 120.47, 120.41, 119.97, 119.70, 119.21, 118.97, 117.05, 116.59, 116.56, 113.71, 68.53, 41.30. HRMS (ESI) calcd for $\text{C}_{22}\text{H}_{18}\text{F}_3\text{N}_2\text{O}_2$, 399.1320 $[\text{M} + \text{H}]^+$; found, 399.1311.

4.1.12. (*E/Z*)-9-((2-(2-Aminoethoxy)pyridin-3-yl)methylene)-*N,N*-dimethyl-9*H*-fluorene-2-carboxamide (**22c**)

The synthesis of compound **22c** was conducted by following a procedure similar to that of compound **5**. The title compound was obtained as a yellow foam. Yield 34 mg, 66%. ^1H NMR (300 MHz, CDCl_3) δ 8.20 (dd, $J = 5.0, 1.9$ Hz, 1H), 7.93–7.88 (m, 1.5H), 7.84–7.81 (m, 0.5H), 7.74–7.69 (m, 2H), 7.60–7.53 (m, 2H), 7.43–7.31 (m, 2.5H), 7.12 (td, $J = 7.6, 1.2$ Hz, 0.5H), 6.98 (ddd, $J = 7.7, 5.0, 3.2$ Hz, 1H), 4.44 (t, $J = 5.3$ Hz, 2H), 3.12–2.93 (m, 8H), 2.65 (s, 2H). HRMS (ESI) calcd for $\text{C}_{24}\text{H}_{24}\text{N}_3\text{O}_2$, 386.1869 $[\text{M} + \text{H}]^+$; found, 383.1858.

4.1.13. (*E/Z*)-2-((3-((2-fluoro-9*H*-fluoren-9-ylidene)methyl)pyridin-2-yl)oxy)ethan-1-amine (**22d**)

The synthesis of compound **22d** was conducted by following a procedure similar to that of compound **5**. The title compound was obtained as a yellow foam. Yield 52 mg, 89%. ^1H NMR (300 MHz, CDCl_3) δ 8.24–8.21 (m, 1H), 7.93–7.87 (m, 1H), 7.81–7.78 (m, 0.5H), 7.65–7.58 (m, 2.5H), 7.53–7.46 (m, 1.5H), 7.40–7.29 (m, 1.5H), 7.20 (dd, $J = 9.9, 2.4$ Hz, 0.5H), 7.10–6.96 (m, 2.5H), 4.48–4.43 (m, 2H), 3.10–3.06 (m, 2H), 2.56 (s, 2H). ^{13}C NMR (75 MHz, CDCl_3) δ 162.78 (d, $J = 272$ Hz), 162.00 (d, $J = 272$ Hz), 161.13, 147.31, 147.17, 141.44, 141.33, 140.61, 139.51, 139.40, 139.27, 139.24, 138.38, 138.13, 138.01, 137.40, 137.37, 136.76, 136.72, 136.68, 136.44, 136.41, 135.13, 135.10, 128.93, 128.56, 126.76, 126.36, 124.05, 122.58, 122.36, 120.72,

120.65, 120.60, 120.57, 120.54, 119.57, 119.34, 119.29, 119.18, 116.73, 116.66, 115.60 (d, $J = 23$ Hz), 115.32 (d, $J = 23$ Hz), 111.30 (d, $J = 24$ Hz), 107.87 (d, $J = 24$ Hz), 68.16, 68.08, 41.14, 41.09. ^{19}F NMR (282 MHz, CDCl_3) δ -114.75, -114.89. HRMS (ESI) calcd for $\text{C}_{21}\text{H}_{18}\text{FN}_2\text{O}$, 333.1403 $[\text{M} + \text{H}]^+$; found, 333.1396.

4.1.14. (*E/Z*)-2-((3-((2-(Trifluoromethyl)-9H-fluoren-9-ylidene)methyl)pyridin-2-yl)oxy)ethan-1-amine (**22e**)

The synthesis of compound **22e** was conducted by following a procedure similar to that of compound **5**. The title compound was obtained as a pale yellow foam. Yield 45 mg, 82%. ^1H NMR (300 MHz, CDCl_3) δ 8.25–8.22 (m, 1H), 8.03 (s, 1H), 7.93–7.84 (m, 1.5H), 7.80–7.75 (m, 2.5H), 7.65–7.54 (m, 2.5H), 7.46–7.34 (m, 1.5H), 7.16 (td, $J = 7.7, 1.2$ Hz, 0.5H), 7.00 (ddd, $J = 7.7, 5.0, 3.1$ Hz, 1H), 4.46–4.42 (m, 2H), 3.07–3.02 (m, 2H), 1.82 (s, 2H). ^{13}C NMR (75 MHz, CDCl_3) δ 161.19, 147.60, 147.37, 140.91 (q, $J = 165.6$ Hz), 139.86, 139.53, 139.46, 139.44, 136.99, 136.49, 136.35, 136.25, 129.00, 128.64, 128.21, 127.84, 125.57 (q, $J = 3.8$ Hz), 125.22 (q, $J = 3.8$ Hz), 124.27, 123.18, 123.05, 121.00 (q, $J = 3.9$ Hz), 120.76, 120.57, 120.31, 119.89, 119.70, 119.23, 118.97, 117.59 (q, $J = 3.9$ Hz), 116.66, 116.59, 68.46, 68.43, 41.26, 41.23. HRMS (ESI) calcd for $\text{C}_{22}\text{H}_{18}\text{F}_3\text{N}_2\text{O}$, 383.1371 $[\text{M} + \text{H}]^+$; found, 383.1361.

4.1.15. (*E/Z*)-9-((2-(2-Aminoethoxy)pyridin-3-yl)methylene)-9H-fluoren-2-ol (**23**)

To the solution of **22a** (33 mg, 0.1 mmol) in CH_2Cl_2 (2 mL) was slowly added BBr_3 (0.3 mL, 0.3 mmol). The reaction was stirred at rt overnight and then treated with saturated NaHCO_3 (aq., 5 mL). The mixture was extracted with CH_2Cl_2 (3×10 mL), dried over Na_2SO_4 , filtered, concentrated and purified by silica gel column chromatography ($\text{CH}_2\text{Cl}_2/\text{MeOH}$) to give compound **23** as a pale-yellow foam. Yield 23 mg, 71%. ^1H NMR (300 MHz, CDCl_3) δ 8.17 (dd, $J = 5.1, 1.8$ Hz, 0.5H), 8.09 (dd, $J = 5.1, 1.8$ Hz, 0.5H), 7.90–7.80 (m, 1H), 7.53 (d, $J = 7.5$ Hz, 1H), 7.47–7.30 (m, 3H), 7.26–7.10 (m, 1.5H), 7.00–6.85 (m, 2H), 6.81–6.73 (m, 1H), 4.42 (t, $J = 5.1$ Hz, 2H), 3.87 (s, 3H), 3.08–2.95 (m, 2H). ^{13}C NMR (75 MHz, CDCl_3) δ 160.89, 160.82, 156.84, 156.31, 146.70, 146.52, 141.83, 141.08, 139.67, 139.64, 139.57, 138.79, 138.02, 137.54, 136.07, 133.59, 131.49, 128.79, 128.47, 125.71, 125.25, 123.82, 120.70, 120.58, 120.30, 120.04, 119.82, 118.92, 118.65, 116.80, 116.49, 116.29, 111.64, 107.76, 67.45, 67.33, 40.90, 40.73. HRMS (ESI) calcd for $\text{C}_{21}\text{H}_{19}\text{N}_2\text{O}_2$, 331.1447 $[\text{M} + \text{H}]^+$; found, 331.1437.

4.1.16. 2-(Difluoromethyl)-9H-fluorene (**25**)

To a solution of 9H-fluorene-2-carbaldehyde (194 mg, 1.0 mmol) in CH_2Cl_2 (3 mL) was slowly added DAST (272 mg, 2.4 mmol) at 0°C . The reaction was stirred at rt overnight and then concentrated and purified by silica gel column chromatography (Hexane) to give **25** as a white solid. Yield: 34%. ^1H NMR (300 MHz, CDCl_3) δ 7.88–7.53 (m, 2H), 7.72 (s, 1H), 7.61–7.52 (m, 2H), 7.46–7.36 (m, 2H), 6.74 (t, $J = 56.7$ Hz, 1H), 3.96 (s, 2H).

4.1.17. (*E/Z*)-2-((3-((2-(Difluoromethyl)-9H-fluoren-9-ylidene)methyl)pyridin-2-yl)oxy)ethan-1-amine (**26**)

Compound **26** was prepared from compound **25** in 72% yield (65 mg) by a procedure similar to that used to prepare compound **5** from compound **4**. The title compound was obtained as a yellow foam. ^1H NMR (300 MHz, CDCl_3) δ 8.24 (dt, $J = 4.9, 2.4$ Hz, 1H), 7.95–7.83 (m, 2H), 7.76 (dd, $J = 8.1, 5.8$ Hz, 2H), 7.67 (s, 0.5H), 7.62–7.34 (m, 4H), 7.15 (t, $J = 7.6$ Hz, 0.5H), 7.02–6.95 (m, 1H), 6.74 (d, $J = 12.8$ Hz, 0.5H), 6.56 (d, $J = 12.8$ Hz, 0.5H), 4.45 (t, $J = 5.3$ Hz, 2H), 3.06 (s, 2H), 1.66 (brs, 2H). ^{13}C NMR (75 MHz, CDCl_3) δ 161.23, 147.41, 147.24, 143.48, 143.46, 143.43, 141.29, 141.26, 141.23, 140.26, 139.71, 139.56, 139.48, 138.10, 136.88, 136.61, 136.55, 133.35, 133.06, 132.87, 132.76, 132.58, 132.29, 128.90, 128.55, 127.85, 127.48, 126.12,

126.04, 125.96, 125.81, 125.73, 125.65, 124.22, 122.62, 122.56, 121.47, 121.39, 121.30, 120.67, 120.36, 120.29, 120.10, 120.02, 119.94, 119.79, 119.71, 119.38, 119.21, 118.24, 118.03, 117.89, 117.81, 117.73, 116.60, 116.57, 115.08, 114.87, 111.92, 111.70, 68.58, 41.30. ^{19}F NMR (282 MHz, CDCl_3) δ -109.20, -109.30, -109.40, -109.50. HRMS (ESI) calcd for $\text{C}_{22}\text{H}_{19}\text{F}_2\text{N}_2\text{O}$, 365.1465 $[\text{M} + \text{H}]^+$; found, 365.1456.

4.1.18. (*E/Z*)-9-((2-(2-Aminoethoxy)pyridin-3-yl)methylene)-9H-fluoren-2-amine (**30a**)

Compound **28** was synthesized following a literature procedure [24]. To a solution of compound **28** (63 mg, 0.2 mmol) in 10 mL of THF was added 0.4 mL of saturated NH_4Cl and 0.4 mL of H_2O . Then Zinc powder (260 mg, 4.0 mmol) was added at 0°C and the reaction was stirred at rt for 2 h. The Zinc solid was filtrated, and the filtrate was concentrated under vacuum to give compound **29** as a yellow solid in 98% yield.

To a solution of **29** (43 mg, 0.1 mmol) in CH_2Cl_2 (2 mL) was slowly added TFA (342 mg, 3.0 mmol). The reaction was stirred at rt overnight and then treated with saturated NaHCO_3 (5 mL). The mixture was extracted with CH_2Cl_2 (3×10 mL), dried over Na_2SO_4 , filtered, concentrated and purified by silica gel column chromatography ($\text{CH}_2\text{Cl}_2/\text{MeOH}$) to give **30a** as a pale-yellow foam. Yield 26 mg, 78%. ^1H NMR (300 MHz, CDCl_3) δ 8.15 (td, $J = 4.8, 1.9$ Hz, 1H), 7.87 (dd, $J = 7.4, 1.9$ Hz, 1H), 7.68 (d, $J = 7.5$ Hz, 0.53H), 7.52–7.37 (m, 3.47H), 7.31–7.25 (m, 0.53H), 7.20 (q, $J = 8.2$ Hz, 1H), 7.09 (d, $J = 2.0$ Hz, 0.47H), 6.95–6.89 (m, 1.47H), 6.78 (d, $J = 2.1$ Hz, 0.53H), 6.62 (td, $J = 8.0, 2.1$ Hz, 1H), 4.39 (q, $J = 3.7, 2.2$ Hz, 2H), 3.27 (s, 4H), 3.04–3.01 (m, 2H). ^{13}C NMR (75 MHz, CDCl_3) δ 161.12, 161.07, 146.75, 146.72, 146.18, 145.58, 142.07, 141.00, 139.82, 139.56, 138.69, 138.01, 137.70, 137.61, 135.90, 132.77, 130.61, 128.77, 128.42, 125.48, 125.05, 123.86, 120.72, 120.66, 120.57, 120.48, 120.28, 119.96, 119.88, 118.61, 118.34, 116.68, 116.64, 115.79, 115.59, 110.90, 107.22, 67.97, 67.74, 41.12, 41.04. HRMS (ESI) calcd for $\text{C}_{21}\text{H}_{20}\text{N}_3\text{O}$, 330.1606 $[\text{M} + \text{H}]^+$; found, 330.1595.

4.1.19. (*E/Z*)-9-((2-(2-Aminoethoxy)pyridin-3-yl)methylene)-*N*-(2-fluoroethyl)-9H-fluoren-2-amine (**30b**)

To a solution of compound **29** (429 mg, 1.0 mmol) in DMF (10 mL) was added 1-bromo-2-fluoroethane (889 mg, 7.0 mmol), K_2CO_3 (695 mg, 5.0 mmol), KI (34 mg, 0.2 mmol). The reaction was stirred at 90°C for 24 h and then diluted with water (50 mL). The mixture was extracted with EtOAc (3×20 mL), dried over Na_2SO_4 , filtered, and concentrated purified by silica gel column chromatography (hexane/ EtOAc) to give 225 mg of the intermediate.

The intermediate (48 mg, 0.1 mmol) was dissolved in CH_2Cl_2 (2 mL) was slowly added TFA (342 mg, 3.0 mmol). The reaction was stirred at rt overnight and then treated with saturated NaHCO_3 (5 mL). The mixture was extracted with CH_2Cl_2 (3×10 mL), dried over Na_2SO_4 , filtered, concentrated and purified by silica gel column chromatography ($\text{CH}_2\text{Cl}_2/\text{MeOH}$) to give **30b** as a pale-yellow foam. Yield 33 mg, 88%. ^1H NMR (300 MHz, CDCl_3) δ 8.23–8.20 (m, 1H), 7.97–7.91 (m, 1H), 7.75–7.72 (m, 0.5H), 7.57–7.42 (m, 3.5H), 7.33 (td, $J = 7.5, 1.2$ Hz, 0.5H), 7.26–7.20 (m, 1H), 7.09 (d, $J = 2.1$ Hz, 0.5H), 7.01–6.93 (m, 1.5H), 6.80 (d, $J = 2.1$ Hz, 0.5H), 6.68 (dd, $J = 8.2, 2.1$ Hz, 0.5H), 6.62 (dd, $J = 8.2, 2.1$ Hz, 0.5H), 4.77 (t, $J = 4.9$ Hz, 0.5H), 4.64–4.60 (m, 1H), 4.48–4.42 (m, 2.5H), 3.57 (dt, $J = 26.5, 4.8$ Hz, 1H), 3.28 (dt, $J = 26.5, 4.8$ Hz, 1H), 3.07 (t, $J = 5.3$ Hz, 2H), 1.78 (s, 2H). ^{13}C NMR (75 MHz, CDCl_3) δ 161.30, 161.21, 147.39, 146.84, 146.77, 146.73, 142.05, 141.02, 139.89, 139.57, 139.46, 138.68, 138.11, 137.82, 137.73, 135.96, 132.36, 130.25, 128.77, 128.44, 125.40, 125.01, 123.90, 120.73, 120.70, 120.57, 120.29, 119.98, 119.88, 118.58, 118.33, 116.60, 116.39, 114.03, 113.78, 108.71, 105.19, 82.47 (d, $J = 166$ Hz), 82.22 (d, $J = 166$ Hz), 68.47, 68.37, 44.61 (d, $J = 166$ Hz), 44.30 (d, $J = 166$ Hz), 41.33. HRMS (ESI) calcd for $\text{C}_{23}\text{H}_{23}\text{FN}_3\text{O}$, 376.1825 $[\text{M} + \text{H}]^+$; found, 376.1815.

4.1.20. (*E/Z*)-*N*-(9-((2-(2-Aminoethoxy)pyridin-3-yl)methylene)-9*H*-fluoren-2-yl)-2-hydroxyacetamide (**30c**)

To a solution of compound **29** (43 mg, 0.1 mmol) in CH₂Cl₂ (2 mL) was added HOBt (15 mg, 0.1 mmol), EDCI (39 mg, 0.2 mmol) and DMAP (2.5 mg, 0.02 mmol). The reaction was stirred at rt overnight and then diluted with water (10 mL). The mixture was extracted with CH₂Cl₂ (3 × 5 mL), dried over Na₂SO₄, filtered, and concentrated *in vacuo* to provide the intermediate, which was used directly in the next step without further purification.

The intermediate was dissolved in CH₂Cl₂ (2 mL) was slowly added TFA (342 mg, 3.0 mmol). The reaction was stirred at rt overnight and then treated with saturated NaHCO₃ (5 mL). The mixture was extracted with CH₂Cl₂ (3 × 10 mL), dried over Na₂SO₄, filtered, concentrated and purified by silica gel column chromatography (CH₂Cl₂/MeOH) to give **30c** as a pale-yellow foam. Yield 18 mg, 46% (two steps). ¹H NMR (300 MHz, CDCl₃) δ 8.88 (s, 0.35H), 8.64 (s, 0.65H), 8.17–8.15 (m, 1H), 8.06 (d, *J* = 1.8 Hz, 0.35H), 7.89–7.85 (m, 1.0H), 7.77–7.73 (m, 1.35H), 7.61–7.43 (m, 3.3H), 7.39–7.23 (m, 2.65H), 7.06–6.92 (m, 1.35H), 4.41–4.39 (m, 2H), 4.13 (s, 0.7H), 4.05 (s, 1.3H), 3.02 (s, 5H). ¹³C NMR (75 MHz, CDCl₃) δ 170.82, 170.62, 160.90, 160.73, 146.88, 141.06, 140.11, 139.61, 139.50, 139.25, 138.84, 137.68, 137.38, 137.11, 137.05, 136.59, 136.41, 136.00, 135.43, 128.82, 128.50, 126.72, 126.25, 123.92, 121.65, 121.37, 120.62, 120.43, 120.13, 120.10, 119.92, 119.60, 119.47, 119.33, 117.06, 116.77, 116.02, 112.27, 67.46, 62.06, 62.02, 40.96, 40.87. HRMS (ESI) calcd for C₂₃H₂₂N₃O₃, 388.1661 [M + H]⁺; found, 388.1654.

4.1.21. (*E/Z*)-*N*-(9-((2-(2-Aminoethoxy)pyridin-3-yl)methylene)-9*H*-fluoren-2-yl)-2-fluoropropanamide (**30d**)

Compound **30d** was prepared by a procedure similar to that used to prepare compound **30c** from compound **29**. The title compound was obtained as a yellow foam. Yield 52 mg, 49% (two steps). ¹H NMR (300 MHz, CDCl₃) δ 8.36 (d, *J* = 6.3 Hz, 0.5H), 8.23–8.11 (m, 2H), 7.97 (dd, *J* = 7.3, 1.9 Hz, 0.5H), 7.89–7.86 (m, 1H), 7.79–7.76 (m, 0.5H), 7.65–7.61 (m, 2H), 7.55 (s, 0.5H), 7.52–7.46 (m, 2H), 7.39–7.27 (m, 1.5H), 7.08–7.00 (m, 1H), 6.94 (dd, *J* = 7.3, 5.0 Hz, 0.5H), 5.23 (q, *J* = 6.8 Hz, 0.25H), 5.15 (q, *J* = 6.8 Hz, 0.25H), 5.07 (q, *J* = 6.8 Hz, 0.25H), 4.98 (q, *J* = 6.8 Hz, 0.25H), 4.45–4.39 (m, 2H), 3.07–3.03 (m, 2H), 1.94 (s, 2H), 1.74 (d, *J* = 6.8 Hz, 0.75H), 1.68–1.65 (m, 1.5H), 1.59 (d, *J* = 6.8 Hz, 0.75H). ¹³C NMR (75 MHz, CDCl₃) δ 168.82, 168.58, 168.34, 161.17, 161.13, 147.08, 146.98, 140.87, 140.24, 139.55, 139.51, 139.45, 138.66, 138.17, 137.11, 136.98, 136.84, 136.58, 136.08, 135.94, 135.41, 128.79, 128.44, 126.81, 126.42, 124.05, 122.10, 122.01, 120.90, 120.46, 120.28, 120.13, 119.98, 119.61, 119.56, 119.35, 119.30, 116.80, 116.59, 116.32, 112.62, 88.93 (d, *J* = 183 Hz), 88.85 (d, *J* = 184 Hz), 68.32, 68.26, 41.32, 41.21, 18.60, 18.31. HRMS (ESI) calcd for C₂₄H₂₃N₃O₂, 404.1774 [M + H]⁺; found, 404.1761.

4.1.22. (*E/Z*)-*N*-(9-((2-(2-Aminoethoxy)pyridin-3-yl)methylene)-9*H*-fluoren-2-yl)cyclopropanesulfonamide (**30e**)

To a solution of compound **29** (86 mg, 0.2 mmol) in CH₂Cl₂ (3 mL) was added cyclopropanesulfonyl chloride (42 mg, 0.3 mmol). The reaction mixture was stirred at rt for 2 h. Water was added and the mixture was extracted with CH₂Cl₂ (3 × 10 mL), dried over Na₂SO₄, filtered, concentrated *in vacuo*. The intermediate was directly used in the next step without further purification.

The intermediate was dissolved in CH₂Cl₂ (2 mL) was slowly added TFA (342 mg, 3.0 mmol). The reaction was stirred at rt overnight and then treated with saturated NaHCO₃ (5 mL). The mixture was extracted with CH₂Cl₂ (3 × 10 mL), dried over Na₂SO₄, filtered, concentrated and purified by silica gel column chromatography (CH₂Cl₂/MeOH) to give **30e** as a pale-yellow foam. Yield 67 mg, 78% (two steps). ¹H NMR (300 MHz, CDCl₃) δ 8.12 (dd, *J* = 5.0, 1.9 Hz, 1H), 7.88 (dd, *J* = 7.3, 1.8 Hz, 0.5H), 7.80 (dd, *J* = 7.3, 1.8 Hz, 0.5H), 7.77–7.70 (m, 1H), 7.60–7.49 (m, 3H), 7.46 (s, 0.5H),

7.38–7.24 (m, 2.5H), 7.21 (dd, *J* = 8.1, 2.0 Hz, 0.5H), 7.04 (td, *J* = 7.6, 1.1 Hz, 0.5H), 6.93 (ddd, *J* = 9.7, 7.3, 5.0 Hz, 1H), 4.46 (q, *J* = 5.7 Hz, 2H), 3.15 (dt, *J* = 21.9, 5.0 Hz, 2H), 2.52 (tt, *J* = 8.0, 4.8 Hz, 0.5H), 2.35 (tt, *J* = 7.8, 4.8 Hz, 0.5H), 1.09 (dt, *J* = 6.9, 3.5 Hz, 1H), 1.00 (dt, *J* = 6.9, 3.4 Hz, 1H), 0.90–0.80 (m, 2H). ¹³C NMR (75 MHz, CDCl₃) δ 160.51, 146.87, 146.80, 140.86, 140.54, 139.80, 139.59, 139.13, 138.50, 138.42, 137.30, 137.12, 136.71, 136.63, 136.23, 136.03, 135.86, 128.93, 128.58, 126.99, 126.47, 123.88, 122.74, 122.02, 121.98, 121.64, 120.60, 120.36, 120.14, 119.74, 119.46, 119.43, 118.61, 118.21, 117.33, 116.99, 114.75, 65.86, 65.06, 40.55, 40.07, 29.79, 29.69, 5.43. HRMS (ESI) calcd for C₂₄H₂₄N₃O₃S, 434.1538 [M + H]⁺; found, 434.1530.

4.1.23. (*E/Z*)-3-((9-((2-(2-Aminoethoxy)pyridin-3-yl)methylene)-9*H*-fluoren-2-yl)amino)-3-methylbutan-1-ol (**32**)

Compound **31** was synthesized from 2-nitro-9*H*-fluorene and 3-methylbut-3-en-1-ol following a literature procedure [31]. Yield 153 mg, 57%. ¹H NMR (300 MHz, Chloroform-*d*) δ 7.69 (dt, *J* = 7.6, 0.9 Hz, 1H), 7.62 (d, *J* = 8.1 Hz, 1H), 7.51 (dt, *J* = 7.4, 0.9 Hz, 1H), 7.36 (td, *J* = 7.5, 1.2 Hz, 1H), 7.25 (td, *J* = 7.4, 1.2 Hz, 1H), 7.12 (d, *J* = 2.0 Hz, 1H), 6.91 (dd, *J* = 8.2, 2.1 Hz, 1H), 3.96 (t, *J* = 5.9 Hz, 2H), 3.86 (s, 2H), 3.55 (s, 1H), 1.94 (t, *J* = 5.9 Hz, 2H), 1.34 (s, 6H).

The synthesis of compound **32** from **31** was conducted by following a procedure similar to that used to prepare compound **5** from compound **4**. The title compound was obtained as a yellow foam. Yield 31 mg, 36% (two steps). ¹H NMR (300 MHz, CDCl₃) δ 8.21–8.17 (m, 1H), 7.93 (dd, *J* = 7.4, 1.9 Hz, 0.4H), 7.82 (dd, *J* = 7.3, 2.0 Hz, 0.6H), 7.72 (d, *J* = 7.5 Hz, 0.6H), 7.55 (t, *J* = 7.0 Hz, 1H), 7.51–7.40 (m, 2.4H), 7.34–7.22 (m, 2H), 7.02–6.95 (m, 1.4H), 6.87 (dd, *J* = 8.1, 2.0 Hz, 0.4H), 6.83 (d, *J* = 2.2 Hz, 0.6H), 6.65 (dd, *J* = 8.2, 2.2 Hz, 0.6H), 4.45–4.38 (m, 1H), 3.89 (t, *J* = 6.2 Hz, 0.8H), 3.67 (t, *J* = 6.7 Hz, 1.2H), 3.24 (s, 4H), 3.07–2.98 (m, 2H), 1.94 (t, *J* = 6.2 Hz, 0.8H), 1.68 (t, *J* = 6.7 Hz, 1.2H), 1.34 (s, 2.4H), 1.13 (s, 3.6H). ¹³C NMR (75 MHz, CDCl₃) δ 161.01, 160.89, 146.74, 146.53, 145.50, 145.36, 141.79, 140.45, 139.87, 139.50, 139.38, 138.61, 138.39, 137.64, 137.55, 136.07, 132.90, 132.01, 128.82, 128.50, 125.56, 125.40, 123.87, 120.62, 120.36, 120.33, 120.30, 120.26, 120.19, 120.01, 119.85, 119.58, 118.92, 118.48, 116.93, 116.74, 112.95, 111.84, 67.43, 59.78, 59.10, 54.83, 53.78, 43.12, 42.09, 40.91, 40.72, 29.69, 28.66, 28.42. HRMS (ESI) calcd for C₂₆H₃₀N₃O₂, 416.2338 [M + H]⁺; found, 416.2328.

4.1.24. (*E/Z*)-3-((3-((2-fluoro-9*H*-fluoren-9-ylidene)methyl)pyridin-2-yl)oxy)propan-1-amine (**35a**)

To a solution of 2-fluoronicotinaldehyde (250 mg, 2.0 mmol) and *tert*-butyl (3-hydroxypropyl)carbamate (700 mg, 4.0 mmol) in DMF (10 mL) was added Na₂CO₃ (424 mg, 4.0 mmol). The reaction mixture was stirred at 110 °C for 12 h, and then water (50 mL) was added. The mixture was extracted with EtOAc (3 × 20 mL), washed with water (3 × 20 mL), dried over Na₂SO₄, filtered, concentrated *in vacuo* and purified by silica gel column chromatography (hexane/ethyl acetate) to give compound **34a** as a colorless oil in 64% yield.

Compound **35a** was prepared from **34a** by a procedure similar to that used to prepare compound **5**. The title compound was obtained as a yellow solid. Yield 23 mg, 54% (two steps). ¹H NMR (300 MHz, CDCl₃) δ 8.24–8.22 (m, 1H), 7.91 (dd, *J* = 10.2, 7.4 Hz, 1H), 7.80 (d, *J* = 7.4 Hz, 0.5H), 7.66–7.47 (m, 4H), 7.40–7.29 (m, 1.5H), 7.21 (dd, *J* = 10.2, 2.3 Hz, 0.5H), 7.10–6.95 (m, 2.5H), 4.53–4.49 (m, 2H), 2.95–2.78 (s, 4H), 2.02–1.93 (m, 2H). ¹³C NMR (75 MHz, CDCl₃) δ 164.42, 163.62, 161.34, 161.18, 160.40, 147.30, 147.17, 141.49, 141.37, 140.62, 139.42, 139.29, 138.38, 138.18, 138.06, 137.41, 136.69, 136.65, 136.61, 136.46, 135.13, 128.85, 128.50, 126.75, 126.31, 124.03, 122.63, 122.43, 120.66, 120.60, 120.53, 120.48, 119.52, 119.34, 119.23, 119.18, 116.54, 116.46, 115.68, 115.43, 115.37, 115.12, 111.45, 111.12, 107.98, 107.66, 63.99, 63.92, 38.69, 32.04, 29.67. HRMS (ESI) calcd for C₂₂H₂₀N₃O, 347.1559 [M + H]⁺; found, 347.1556.

4.1.25. (*E/Z*)-2-((3-((2-fluoro-9H-fluoren-9-ylidene)methyl)pyridin-2-yl)oxy)-*N*-methylethan-1-amine (**35b**)

To a solution of compound 2-fluoronicotinaldehyde (125 mg, 1.0 mmol) in 3 mL of THF was added NaH (40 mg, 1.0 mmol). After stirred at 0 °C for 10 min, *tert*-butyl (2-hydroxyethyl)(methyl) carbamate (175 mg, 1.0 mmol) was added and the reaction was stirred at 0 °C for 30 min. Ice water (20 mL) was added and the reaction was extracted with CH₂Cl₂ (3 × 10 mL). The combined organic layer was washed with water, dried over Na₂SO₄, filtered, and concentrated *in vacuo*. The residue was purified by silica column chromatography (MeOH/CH₂Cl₂, 1:20) to give compound **34b** as a yellow oil in 15% yield.

Compound **35b** was prepared from **34b** by a procedure similar to that used to prepare compound **5**. The title compound was obtained as a yellow solid. Yield 26 mg, 77% (two steps). ¹H NMR (300 MHz, CDCl₃) δ 8.25–8.22 (m, 1H), 7.94–7.87 (m, 1H), 7.80 (d, *J* = 7.2 Hz, 0.5H), 7.67–7.61 (m, 2H), 7.58 (s, 0.5H), 7.53–7.45 (m, 1.5H), 7.39–7.28 (m, 1.5H), 7.20 (dd, *J* = 10.0, 2.4 Hz, 0.5H), 7.11–6.96 (m, 2.5H), 4.57–4.52 (m, 2H), 2.99–2.94 (m, 2H), 2.44 and 2.42 (s, 3H). ¹³C NMR (75 MHz, CDCl₃) δ 164.41, 163.64, 161.21, 161.18, 160.42, 147.35, 147.22, 141.49, 141.38, 140.59, 139.43, 139.33, 139.30, 138.41, 138.19, 138.07, 137.38, 137.35, 136.76, 136.71, 136.67, 136.49, 136.46, 135.16, 135.13, 128.88, 128.52, 126.73, 126.37, 124.07, 122.68, 122.43, 120.67, 120.63, 120.55, 120.52, 119.53, 119.33, 119.27, 119.17, 116.63, 116.54, 115.71, 115.44, 115.40, 115.13, 111.48, 111.15, 107.97, 107.66, 65.57, 50.59, 36.24. HRMS (ESI) calcd for C₂₂H₂₀FN₂O, 347.1559 [M + H]⁺; found, 347.1556.

4.1.26. (*E/Z*)-*N*¹-(3-((2-fluoro-9H-fluoren-9-ylidene)methyl)pyridin-2-yl)-*N*¹-methylethane-1,2-diamine (**35c**)

To a solution of 2-fluoronicotinaldehyde (250 mg, 1.0 mmol) and *tert*-butyl (2-(methylamino)ethyl)carbamate (209 mg, 1.2 mmol) in MeCN (10 mL) was added K₂CO₃ (207 mg, 1.5 mmol). The reaction mixture was stirred at 80 °C for 3 h, and then water (20 mL) was added. The mixture was extracted with EtOAc (3 × 20 mL), washed with water (3 × 20 mL), dried over Na₂SO₄, filtered, concentrated *in vacuo* and purified by silica gel column chromatography (hexane/ethyl acetate) to give compound **34c** as a colorless oil in 42% yield.

Compound **35c** was prepared from **34c** by a procedure similar to that used to prepare compound **5**. The title compound was obtained as a yellow foam. Yield 35 mg, 61% (two steps). ¹H NMR (300 MHz, CDCl₃) δ 8.30–8.27 (m, 1H), 7.86–7.79 (m, 1.5H), 7.70–7.64 (m, 2.5H), 7.54–7.47 (m, 1.5H), 7.41–7.30 (m, 2H), 7.15–7.02 (m, 1.5H), 6.89–6.83 (m, 1H), 3.51–3.46 (m, 2H), 3.01–2.97 (m, 5H), 2.62 (brs, 2H). ¹³C NMR (75 MHz, CDCl₃) δ 164.46, 163.72, 161.23, 160.66, 160.50, 147.71, 147.59, 141.49, 141.38, 140.38, 140.00, 139.86, 139.31, 139.29, 138.23, 138.20, 138.09, 137.16, 137.13, 136.51, 136.48, 134.98, 134.95, 134.31, 134.27, 134.23, 128.76, 128.37, 126.83, 126.66, 126.48, 124.02, 120.81, 120.75, 120.69, 120.63, 120.29, 120.18, 120.03, 119.63, 119.37, 115.63, 115.32, 115.22, 115.16, 115.01, 111.40, 111.08, 107.66, 107.35, 56.13, 55.98, 39.93, 39.84, 39.50, 39.48. HRMS (ESI) calcd for C₂₂H₂₁FN₃, 346.1719 [M + H]⁺; found, 346.1714.

4.1.27. (*E/Z*)-1-(3-((2-fluoro-9H-fluoren-9-ylidene)methyl)pyridin-2-yl)azetidin-3-amine (**35d**)

To a solution of 2-fluoronicotinaldehyde (250 mg, 2.0 mmol) and *tert*-butyl azetidin-3-ylcarbamate (344 mg, 2.0 mmol) in DMF (10 mL) was added Na₂CO₃ (318 mg, 3.0 mmol). The reaction mixture was stirred at 110 °C for 3 h, and then water (50 mL) was added. The mixture was extracted with EtOAc (3 × 20 mL), washed with water (3 × 20 mL), dried over Na₂SO₄, filtered, concentrated *in vacuo* and purified by silica gel column chromatography (hexane/ethyl acetate) to give compound **34d** as a colorless oil in 78% yield.

Compound **35d** was prepared from **34d** by a procedure similar

to that used to prepare compound **5**. The title compound was obtained as a yellow solid. Yield 36 mg, 41% (two steps). ¹H NMR (300 MHz, CDCl₃) δ 8.26 (d, *J* = 4.9 Hz, 1H), 7.74 (d, *J* = 7.4 Hz, 0.5H), 7.68–7.62 (m, 3H), 7.51–7.31 (m, 3.5H), 7.20 (dd, *J* = 9.9, 2.4 Hz, 0.5H), 7.13–7.00 (m, 1.5H), 6.80–6.74 (m, 1H), 4.31–4.25 (m, 2H), 3.83–3.77 (m, 1H), 3.72–3.65 (m, 2H), 1.71 (brs, 2H). ¹³C NMR (75 MHz, CDCl₃) δ 164.44, 163.69, 161.20, 160.47, 159.02, 158.96, 148.24, 148.12, 141.32, 141.21, 140.34, 139.15, 138.76, 138.67, 138.38, 138.21, 138.09, 137.11, 136.49, 135.53, 135.11, 128.75, 128.50, 126.79, 126.49, 124.67, 124.56, 124.44, 120.77, 120.66, 120.54, 120.09, 119.48, 119.37, 117.07, 116.92, 115.60, 115.41, 115.29, 115.10, 113.83, 113.70, 111.91, 111.58, 107.52, 107.21, 62.85, 44.05, 29.69. HRMS (ESI) calcd for C₂₂H₁₉FN₃, 344.1563 [M + H]⁺; found, 344.1573.

4.1.28. *tert*-Butyl (2-((3-(1,3-dioxolan-2-yl)pyrazin-2-yl)oxy)ethyl)carbamate (**37**)

To a solution of 3-chloropyrazine-2-carbaldehyde (286 mg, 2.0 mmol) in toluene (5 mL) was added ethane-1,2-diol (372 mg, 6.0 mmol) and TsOH (19 mg, 0.1 mmol). The mixture was stirred at 110 °C for 5 h, and then concentrated *in vacuo*. Water was added and the residue was extracted with CH₂Cl₂ (3 × 10 mL), dried over Na₂SO₄, filtered, concentrated to provide the intermediate.

To a solution of the intermediate (186 mg, 1.0 mmol) in THF (5 mL) was added NaH (60 mg, 1.5 mmol) and *tert*-butyl (2-hydroxyethyl)carbamate (322 mg, 2.0 mmol). The mixture was stirred at 50 °C overnight and then quenched with water (10 mL). The residue was extracted with CH₂Cl₂ (3 × 10 mL), dried over Na₂SO₄, filtered, concentrated and purified by silica gel column chromatography (CH₂Cl₂/EtOAc) to give compound **37** as a yellow oil. Yield 150 mg, 41% (two steps). ¹H NMR (300 MHz, CDCl₃) δ 8.16 (d, *J* = 2.7 Hz, 1H), 8.09 (d, *J* = 2.7 Hz, 1H), 6.19 (s, 1H), 5.14 (s, 1H), 4.47 (t, *J* = 5.4 Hz, 2H), 4.30–4.20 (m, 2H), 4.17–4.04 (m, 2H), 3.55 (q, *J* = 5.4 Hz, 2H), 1.45 (s, 9H).

4.1.29. (*E/Z*)-2-((3-((2-fluoro-9H-fluoren-9-ylidene)methyl)pyrazin-2-yl)oxy)ethan-1-amine (**39**)

To a solution of compound **37** (311 mg, 1.0 mmol) in MeOH (5 mL) was added 1 N HCl (5 mL, 5.0 mmol). The mixture was stirred at rt overnight and treated with saturated NaHCO₃ (5 mL). Then the reaction was extracted with CH₂Cl₂ (3 × 10 mL), dried over Na₂SO₄, filtered, concentrated to provide compound **38** as a colorless oil, which was directly used in the next step without further purification.

Compound **39** was prepared from **38** by a procedure similar to that used to prepare compound **5**. The title compound was obtained as a yellow foam. Yield 67 mg, 50% (two steps). ¹H NMR (300 MHz, CDCl₃) δ 8.58–8.51 (m, 1H), 8.36 (dd, *J* = 5.3, 2.7 Hz, 1H), 8.09 (t, *J* = 2.4 Hz, 1H), 7.79 (t, *J* = 3.8 Hz, 1H), 7.65–7.58 (m, 2.5H), 7.47 (dd, *J* = 9.2, 2.3 Hz, 0.5H), 7.40–7.28 (m, 1.5H), 7.21 (td, *J* = 7.7, 1.2 Hz, 0.5H), 7.12–7.04 (m, 1H), 4.50–4.46 (m, 2H), 3.19–3.13 (m, 2H), 1.57 (brs, 2H). ¹³C NMR (75 MHz, CDCl₃) δ 164.40, 164.06, 161.17, 160.85, 158.57, 158.53, 142.19, 142.08, 141.08, 140.62, 140.49, 140.40, 140.36, 140.26, 140.22, 140.13, 140.10, 140.06, 139.12, 138.08, 137.95, 137.92, 137.89, 136.32, 136.29, 136.01, 135.96, 135.86, 135.83, 129.83, 129.14, 127.08, 126.86, 126.73, 120.66, 120.53, 120.19, 120.07, 119.39, 119.29, 119.22, 116.48, 116.17, 115.96, 115.65, 115.09, 114.75, 108.18, 107.86, 69.16, 41.18, 41.12. HRMS (ESI) calcd for C₂₀H₁₇FN₃O, 334.1355 [M + H]⁺; found, 334.1344.

4.1.30. (*E/Z*)-2-aminoethyl-4-((2-fluoro-9H-fluoren-9-ylidene)methyl)pyrazolo[1,5-*a*]pyridine-3-carboxylate (**44a**)

Compounds **41** and **42** were synthesized following a literature procedure [32]. To a solution of 2-fluoro-9H-fluorene (40 mg, 0.22 mmol) in MeOH (5 mL) was added compound **41** (41 mg, 0.2 mmol) and KF·Al₂O₃ (39 mg, 0.24 mmol). The reaction mixture

was stirred at 70 °C for 48 h, and then evaporated under vacuum and purified by silica gel column chromatography (CH₂Cl₂/EtOAc) to give the hydrolyzed product **43** as a yellow solid in 81% yield.

To a solution of compound **43** (86 mg, 0.2 mmol) in CH₂Cl₂ (2 mL) was added EDCl (77 mg, 0.4 mmol), DMAP (5 mg, 0.04 mmol) and *tert*-butyl (2-hydroxyethyl)carbamate (64 mg, 0.4 mmol). The reaction was stirred at rt overnight and then diluted with water (10 mL). The mixture was extracted with CH₂Cl₂ (3 × 5 mL), dried over Na₂SO₄, filtered, and concentrated *in vacuo* to provide the intermediate which was directly used in the next step without further purification.

To a solution of the intermediate in CH₂Cl₂ (4 mL) was slowly added TFA (342 mg, 3.0 mmol). The reaction was stirred at rt overnight and then treated with saturated NaHCO₃ (5 mL). The mixture was extracted with CH₂Cl₂ (3 × 10 mL), dried over Na₂SO₄, filtered, concentrated and purified by silica gel column chromatography (CH₂Cl₂/MeOH) to give **44a** as a pale-yellow solid. Yield 18 mg, 23% (two steps). ¹H NMR (300 MHz, CDCl₃) δ 8.65–8.61 (m, 1H), 8.54 (d, *J* = 2.3 Hz, 1H), 8.38 (s, 0.5H), 8.31 (s, 0.5H), 7.93–7.91 (m, 0.5H), 7.77 (dd, *J* = 11.8, 7.2 Hz, 1H), 7.70–7.59 (m, 2.5H), 7.49 (d, *J* = 7.8 Hz, 0.5H), 7.44–7.31 (m, 1.5H), 7.20–6.99 (m, 3H), 4.27–4.22 (m, 2H), 3.00–2.90 (m, 2H), 1.48 (s, 2H). ¹³C NMR (75 MHz, CDCl₃) δ 166.60, 164.55, 163.49, 162.73, 162.69, 161.32, 160.27, 146.61, 146.55, 141.71, 141.59, 140.99, 139.50, 139.48, 138.95, 138.87, 138.34, 138.01, 137.89, 137.77, 137.74, 136.33, 136.30, 135.64, 135.60, 135.10, 135.07, 129.65, 129.55, 129.51, 129.45, 128.91, 128.69, 128.23, 128.10, 126.99, 126.22, 125.84, 125.68, 124.02, 120.86, 120.83, 120.72, 120.63, 120.52, 119.69, 119.27, 115.78, 115.65, 115.47, 115.34, 113.27, 113.25, 111.46, 111.13, 108.33, 108.02, 105.46, 66.60, 41.10. HRMS (ESI) calcd for C₂₂H₁₉FN₃O₂, 400.1461 [M + H]⁺; found, 400.1467.

4.1.31. (*E/Z*)-*N*-(2-Aminoethyl)-4-((2-fluoro-9H-fluoren-9-ylidene)methyl)pyrazolo[1,5-*a*]pyridine-3-carboxamide (**44b**)

To a solution of compound **43** (86 mg, 0.2 mmol) in CH₂Cl₂ (2 mL) was added HATU (114 mg, 0.3 mmol), HOAt (27 mg, 0.2 mmol). After stirring at rt for 30 min, the *tert*-butyl (2-aminoethyl)carbamate (48 mg, 0.3 mmol) and DIPEA (78 mg, 0.6 mmol) was added. The resulting mixture was stirred at rt overnight and then diluted with water (10 mL). The mixture was extracted with CH₂Cl₂ (3 × 5 mL), dried over Na₂SO₄, filtered, and concentrated *in vacuo* to provide the intermediate which was directly used in the next step without further purification.

The intermediate was dissolved in CH₂Cl₂ (2 mL) was slowly added TFA (342 mg, 3.0 mmol). The reaction was stirred at rt overnight and then treated with saturated NaHCO₃ (5 mL). The mixture was extracted with CH₂Cl₂ (3 × 10 mL), dried over Na₂SO₄, filtered, concentrated and purified by silica gel column chromatography (CH₂Cl₂/MeOH) to give product **44b** as a pale-yellow solid. Yield 37 mg, 46% (two steps). ¹H NMR (300 MHz, CDCl₃) δ 8.59 (dd, *J* = 6.9, 2.5 Hz, 1H), 8.29 (d, *J* = 4.3 Hz, 1H), 8.22 (s, 0.5H), 8.13 (s, 0.5H), 7.90 (d, *J* = 7.3 Hz, 0.5H), 7.68–7.58 (m, 3.5H), 7.48–7.31 (m, 2H), 7.20 (dd, *J* = 9.9, 2.4 Hz, 0.5H), 7.14–6.97 (m, 1.5H), 6.35 (brs, 1H), 3.33–3.27 (m, 2H), 2.67–2.65 (m, 2H), 1.16 (brs, 2H). ¹³C NMR (75 MHz, CDCl₃) δ 164.54, 163.53, 163.48, 163.43, 161.29, 160.30, 143.05, 142.91, 141.48, 141.37, 140.93, 139.25, 138.30, 137.88, 137.76, 137.73, 137.70, 137.17, 137.07, 136.62, 136.58, 136.55, 136.20, 135.07, 135.04, 129.18, 129.07, 129.03, 128.88, 127.71, 127.63, 127.51, 127.08, 126.33, 124.59, 124.49, 124.13, 121.05, 120.83, 120.71, 120.63, 120.51, 119.65, 119.24, 115.95, 115.82, 115.64, 115.51, 112.64, 111.58, 111.26, 110.11, 108.48, 108.16, 42.37, 41.13, 41.10. HRMS (ESI) calcd for C₂₄H₂₀FN₄O, 399.1621 [M + H]⁺; found, 399.1631.

4.1.32. (*E/Z*)-2-aminoethyl-6-((2-fluoro-9H-fluoren-9-ylidene)methyl)pyrazolo[1,5-*a*]pyridine-3-carboxylate (**46a**)

To a solution of 2-fluoro-9H-fluorene (40 mg, 0.22 mmol) in

MeOH (5 mL) was added compound **42** (41 mg, 0.2 mmol) and KF-Al₂O₃ (39 mg, 0.24 mmol). The reaction mixture was stirred at 70 °C for 48 h, and then evaporated under vacuum and purified by silica gel column chromatography (CH₂Cl₂/EtOAc) to give the hydrolyzed product **45** as a yellow solid in 63% yield.

To a solution of compound **45** (86 mg, 0.2 mmol) in CH₂Cl₂ (2 mL) was added HATU (114 mg, 0.3 mmol), HOAt (27 mg, 0.2 mmol). After stirred at rt for 30 min, *tert*-butyl (2-hydroxyethyl)carbamate (48 mg, 0.3 mmol) and DIPEA (78 mg, 0.6 mmol) was added. The resulting mixture was stirred at rt overnight and then refluxed for additional 24 h. After diluted with water (10 mL), the mixture was extracted with CH₂Cl₂ (3 × 5 mL), dried over Na₂SO₄, filtered, and concentrated *in vacuo* to provide the intermediate which was directly used in the next step without further purification.

The intermediate was dissolved in CH₂Cl₂ (2 mL) was slowly added TFA (342 mg, 3.0 mmol). The reaction was stirred at rt overnight and then treated with saturated NaHCO₃ (5 mL). The mixture was extracted with CH₂Cl₂ (3 × 10 mL), dried over Na₂SO₄, filtered, concentrated and purified by silica gel column chromatography (CH₂Cl₂/MeOH) to give product **46a** as a pale-yellow solid. m.p., 176.9–179.2 °C. Yield 18 mg, 21% (two steps). ¹H NMR (300 MHz, CDCl₃) δ 8.74 (d, *J* = 8.1 Hz, 1H), 8.50 (d, *J* = 1.6 Hz, 1H), 8.27 (dd, *J* = 9.1, 4.5 Hz, 1H), 7.78 (d, *J* = 7.5 Hz, 0.5H), 7.69–7.63 (m, 2.5H), 7.58 (s, 0.5H), 7.52–7.32 (m, 3.5H), 7.19–7.03 (m, 2H), 4.43 (t, *J* = 5.4 Hz, 2H), 3.17–3.13 (m, 2H), 1.63 (s, 2H). ¹³C NMR (75 MHz, CDCl₃) δ 164.45, 163.68, 163.24, 163.20, 161.20, 160.44, 145.58, 145.53, 140.96, 140.86, 140.09, 138.80, 138.72, 138.51, 137.73, 137.44, 137.32, 135.77, 135.47, 129.53, 129.24, 129.15, 129.02, 128.93, 126.96, 126.71, 124.26, 123.21, 123.05, 121.79, 121.66, 120.99, 120.88, 120.77, 120.44, 119.79, 119.49, 118.95, 118.77, 116.36, 116.05, 115.75, 111.77, 111.44, 107.97, 107.65, 104.35, 104.25, 66.47, 41.29. HRMS (ESI) calcd for C₂₂H₁₉FN₃O₂, 400.1461 [M + H]⁺; found, 400.1469.

4.1.33. (*E/Z*)-*N*-(2-Aminoethyl)-6-((2-fluoro-9H-fluoren-9-ylidene)methyl)pyrazolo[1,5-*a*]pyridine-3-carboxamide (**46b**)

Compound **46b** was prepared from **45** by a procedure similar to that used to prepare compound **44b** from compound **43**. The title compound was obtained as a yellow solid. Yield 26 mg, 37% (two steps). ¹H NMR (300 MHz, CDCl₃) δ 8.67 (d, *J* = 5.7 Hz, 1H), 8.40 (dd, *J* = 9.1, 5.7 Hz, 1H), 8.29 (d, *J* = 1.8 Hz, 1H), 7.76 (d, *J* = 7.5 Hz, 0.5H), 7.67–7.31 (m, 6.5H), 7.19 (dd, *J* = 9.7, 2.3 Hz, 0.5H), 7.14–7.02 (m, 1.5H), 6.64 (t, *J* = 5.8 Hz, 1H), 3.57 (q, *J* = 5.8 Hz, 2H), 3.01 (t, *J* = 5.9 Hz, 2H), 1.60 (s, 2H). ¹³C NMR (75 MHz, CDCl₃) δ 164.42, 163.68, 163.36, 163.32, 161.18, 160.44, 141.35, 141.29, 141.04, 140.93, 140.87, 139.72, 139.69, 138.88, 138.68, 138.27, 138.23, 137.65, 137.62, 137.50, 137.39, 135.83, 135.80, 135.43, 135.40, 129.41, 129.02, 128.53, 128.45, 128.20, 127.96, 126.89, 126.69, 124.36, 122.89, 122.74, 122.18, 122.03, 120.91, 120.83, 120.79, 120.71, 120.40, 119.71, 119.44, 119.26, 116.25, 115.93, 115.62, 111.81, 111.48, 107.91, 107.66, 107.58, 41.80, 41.51. HRMS (ESI) calcd for C₂₄H₂₀FN₄O, 399.1621 [M + H]⁺; found, 399.1628.

4.2. *In vitro* determination of newly synthesized compounds against cancer cell proliferation

For IC₅₀ calculations, MCF-7, MDA-MB-231 and other breast cancer cell lines were seeded in 96-well plates at a density of 1 × 10³ cells/well and treated with DMSO and 0.1 μM, 0.33 μM, 1 μM, 3.3 μM, and 10 μM of individual compound for 72 h, and then 10 μL of 3-(4,5-dimethylthiazol-2-yl)-2,5-diphenyltetrazolium bromide (MTT) (5 mg/mL in PBS) was added to each well for incubation of 3 h, followed by adding 200 μL of DMSO to each well after removal of MTT solution. Absorbance was determined for all wells by measuring OD at 560 nm after a 10 min incubation on a 96-

well GlowMaxate absorbance reader (Promega, Madison, WI). Each individual compound was measured for designated concentrations in quadruplicate wells.

For cell viability assays, MCF-10A, MCF7, MDA-MB-361, MDA-MB-468, and BT549 were seeded in 96-well plate at a density 1×10^3 cells/well. MDA-MB-231 cells were seeded at 600 cell/well. Each individual compound was measured for designated concentrations in quadruplicate wells and independently repeated three times.

4.3. Colony formation assay

Breast cancer MCF-7 and MDA-MB-231 cells were seeded in 6-well tissue culture plates with a density of 1×10^3 or 600 cells per well, respectively, and maintained in regular culture media. After 24 h, the cells were treated with compound **22d** at varying concentrations (0.1 μ M, 0.2 μ M, 0.3 μ M, 0.5 μ M, and 1 μ M) or DMSO as the vehicle. The culture media with the compounds were changed every 72 h. At the end of 1 week, the wells were washed twice with PBS buffer fixed with 4% paraformaldehyde. Subsequently, the wells were washed twice with PBS and 2 mL of 0.01% crystal violet staining buffer was added to each well and incubated for 10 min. The wells were then washed with PBS for 5 min for three times and allowed to dry. Photographs were taken, and the number of colonies counted by Image J software program. Experiments were performed in triplicates, and the counted data was analyzed with GraphPad Prizm 9 software package. Error bars represent standard deviation.

4.4. Migration and invasion assay

For migration and invasion assays, MDA-MB-231 cells were seeded into 6-well plates (10^5 cells/well). The next day, cells were treated with **22d** at concentrations of 0, 0.1 μ M, 0.5 μ M, and 1 μ M, respectively. After 24 h, cells were trypsinized, washed in PBS ($2 \times$) and counted with the Countess II FL cell counter (Invitrogen). Subsequently, the cells were resuspended in DMEM containing 0.1% FBS and seeded into migration or invasion chambers (Invitrogen) at a density of 10^5 cells in 500 μ L per chamber. A volume of 800 μ L of DMEM containing 10% FBS were added to the well of a 24-well plate and the migration chambers were inserted. The cells were incubated for 8 h (migration) or 16 h (invasion) before they were washed in PBS containing calcium and magnesium ($2 \times$) and fixed in 4% PFA for 15 min at room temperature. After fixation, the cells were washed with H₂O, stained with crystal violet for 15 min at room temperature, and again washed with H₂O to remove excessive dye. To remove cells that were not migrated, the inner part of the chambers was wiped with a wet cotton swap. The chambers were dried overnight, and pictures of the migration and invasion assays were taken with the Echo Revolve microscope with a $10 \times$ magnification. Cell numbers were determined using Image J software program and the cell counter plugin. The assays were performed in triplicates with two biological replicates for each concentration and vehicle control, respectively. Cells were counted in 3 randomly picked areas of the chambers at a $10 \times$ magnification for all replicates which resulted in an average cell count of 6 areas per technical replicate and a total average of 18 counting areas per treatment.

4.5. Mitochondria and cytosol fractionation

For mitochondrial and cytosol fractionation, we used the mitochondrial/cytosol fractionation kit from Abcam (#ab65320) following manufacture's protocol. Briefly, $1-2 \times 10^7$ cells were collected, washed with PBS, and incubated with cytosol extraction

buffer with protease inhibitor for 10 min on ice. After incubation, the cells were homogenized using Dounce homogenizer passing 30–50 times. Homogenized cells were centrifuged at 700 g for 10 min, supernatant transferred to new tubes for centrifugation at 10,000 g 30 min. Supernatants were collected as cytosolic fraction and pellet as mitochondrial fraction.

4.6. Western-blot analysis

Breast cancer MDA-MB-231 cells were treated with DMSO, or compound **22d**. After indicated time of treatment at designated doses, cells were harvested and lysed. Mouse xenograft tumors were grounded and lysed with RIPA buffer using tissue homogenizer (Omni tech). Homogenized lysates were centrifuged at 13,000 rpm at 4 °C for 20 min, and supernatants collected for measuring protein concentration. Protein concentrations were quantified by the method of Bradford with bovine serum albumin as protein standard. Equal amounts of total cellular protein extract (30 μ g) were separated by electrophoresis on SDS–polyacrylamide gels and transferred to PVDF membranes. After blocking with 5% nonfat milk, the membrane was incubated with the desired primary antibody overnight at the following dilutions: anti-Bax (1:1,000, ab32503), anti-pBax (1:500, Sigma SAB4504690), anti-cytochrome C (1:1,000, CST11940), anti-PARP-1 (1:1,000, ab32138), anti-cleaved PARP-1 (1:1,000, CST5625), caspase 3 (1:1,000, CST #14220), cleaved Caspase 3 (1:1,000, CST #9664), and β -actin (1:20,000, Sigma A5441). Subsequently, the membranes were incubated with appropriate secondary antibody. The immunoreactive bands were visualized by enhanced chemiluminescence (Thermo, 32106) as recommended by the manufacturer. Signals were detected with the ChemiDoc MP Imaging System (BIO-RAD).

4.7. In vivo antitumor activity determination

Female nude mice were purchased from Charles River Laboratory. All animals were maintained at the Louisiana Cancer Research Center animal facilities according to the NIH guidelines and all procedures were approved by the institutional IACUC. The mice were maintained in a barrier unit with 12 h light–dark switch. At 6 weeks of age, the mice were randomized into two groups for intraperitoneal (I.P.) injection and intratumoral (I.T.) injection and MDA-MB-231 cells were administered into the 3rd mammary fat pad (5×10^5 cells per mouse in 100 μ L PBS). The tumor development was observed, and treatment was started when tumor volume reached 100 mm³. The tumor volume was estimated using the following formula: Volume = (width² \times length)/2.

For I.P. injection studies, the mice were randomly divided into three groups: DMSO control, 10 mg/kg treatment, and 20 mg/kg, and then mice were treated daily. For I.T. injection, the animals were randomly divided into two groups, one control group and one treatment group with 15 mg/kg dose. Mice were treated every other day. In both I.P. and I.T., tumor volume and body weight were measured daily. The compound **22d** was dissolved in a mixture of DMSO and PEG-400 (1:1). The mixture of DMSO and PEG-400 without supplement was used as vehicle control. The mice were treated daily for 10 days with **22d** or vehicle at indicated concentration via I.P. or I.T. administration and the mice were sacrificed when the tumor volume reached 2000 mm³. To ensure comparability, the treatment period of the first mouse sacrificed was set as the overall treatment time and the remaining mice were sacrificed after same amount of time after starting the treatment. In each group, tumors of all mice were collected for later protein extraction.

4.8. Molecular docking method

The molecular docking study was performed with Small Molecule Drug Discovery Suite (Schrödinger Release 2020-4, Schrödinger, LLC, New York, NY, 2019). NMR Solution structure of Bax (PDB ID: 1F16) was obtained from RCSB PDB bank. The average structure analysis was performed on all conformations and one representative structure was selected. The selected structure was preprocessed and optimized with Schrödinger Protein Preparation Wizard. The grid box in 20 Å was generated using Glide Grid and the grid box was centered on the residues of S184 site ($x = -9.253$, $y = -6.165$, $z = 8.697$). Compound **22d** was created with Maestro and prepared with LigPrep to generate a suitable 3-D conformation for docking. Ligand docking was performed with Glide using SP mode with default settings. The docked pose was incorporated into Maestro pose viewer to visualize the interaction on the binding site.

Declaration of competing interest

The authors declare that they have no known competing financial interests or personal relationships that could have appeared to influence the work reported in this paper.

Acknowledgments

This work was supported by Breast Cancer Research Program (BCRP) Breakthrough Award W81XWH-17-1-0071 (to J.Z.) and W81XWH-17-1-0072 (to Q.S.) from the Department of Defense (DoD), USA. J.Z. is also partly supported by the John D. Stobo, M.D. Distinguished Chair Endowment Fund at UTMB.

Appendix A. Supplementary data

Supplementary data to this article can be found online at <https://doi.org/10.1016/j.ejmech.2021.113427>.

References

- [1] S. Elmore, Apoptosis: a review of programmed cell death, *Toxicol. Pathol.* 35 (2007) 495–516.
- [2] R.S. Wong, Apoptosis in cancer: from pathogenesis to treatment, *J. Exp. Clin. Oncol.* 30 (2011) 87.
- [3] M. Hassan, H. Watari, A. AbuAlmaaty, Y. Ohba, N. Sakuragi, Apoptosis and molecular targeting therapy in cancer, *BioMed Res. Int.* 2014 (2014) 150845.
- [4] A.N. Hata, J.A. Engelman, A.C. Faber, The BCL2 family: key mediators of the apoptotic response to targeted anticancer therapeutics, *Canc. Discov.* 5 (2015) 475–487.
- [5] Z. Liu, H. Chen, J. Zhou, Apoptosis regulator BAX, in: S. Choi (Ed.), *Encyclopedia of Signaling Molecules*, Springer New York, New York, NY, 2016, pp. 1–6.
- [6] F. Edlich, S. Banerjee, M. Suzuki, M.M. Cleland, D. Arnoult, C. Wang, A. Neutzner, N. Tjandra, R.J. Youle, Bcl-x(L) retrotranslocates Bax from the mitochondria into the cytosol, *Cell* 145 (2011) 104–116.
- [7] L.D. Walensky, E. Gavathiotis, BAX unleashed: the biochemical transformation of an inactive cytosolic monomer into a toxic mitochondrial pore, *Trends Biochem. Sci.* 36 (2011) 642–652.
- [8] Z. Liu, Y. Ding, N. Ye, C. Wild, H. Chen, J. Zhou, Direct activation of bax protein for cancer therapy, *Med. Res. Rev.* 36 (2016) 313–341.
- [9] L.A. Torre, F. Bray, R.L. Siegel, J. Ferlay, J. Lortet-Tieulent, A. Jemal, Global cancer statistics, *CA A Cancer J. Clin.* 65 (2012) 87–108, 2015.
- [10] N. Harbeck, M. Gnant, Breast cancer, *Lancet* 389 (2017) 1134–1150.
- [11] T.A. Moo, R. Sanford, C. Dang, M. Morrow, Overview of breast cancer therapy, *Pet. Clin.* 13 (2018) 339–354.
- [12] A.Y. Michaels, A.R. Keraliya, S.H. Tirumani, A.B. Shinagare, N.H. Ramaiya, Systemic treatment in breast cancer: a primer for radiologists, *Insights Imag.* 7 (2016) 131–144.
- [13] A.G. Waks, E.P. Winer, Breast cancer treatment: a review, *J. Am. Med. Assoc.* 321 (2019) 288–300.
- [14] P. Pluta, P. Smolewski, A. Pluta, B. Cebula-Obrzut, A. Wierzbowska, D. Nejc, T. Robak, R. Kordek, L. Gottwald, J. Piekarski, A. Jeziorski, Significance of Bax expression in breast cancer patients, *Pol. Przegl. Chir.* 83 (2011) 549–553.
- [15] I.R. Bukholm, G. Bukholm, J.M. Nesland, Reduced expression of both Bax and Bcl-2 is independently associated with lymph node metastasis in human breast carcinomas, *APMIS* 110 (2002) 214–220.
- [16] S. Krajewski, C. Blomqvist, K. Franssila, M. Krajewska, V.-M. Wasenius, E. Niskanen, S. Nordling, J.C. Reed, Reduced expression of proapoptotic gene BAX is associated with poor response rates to combination chemotherapy and shorter survival in women with metastatic breast adenocarcinoma, *Canc. Res.* 55 (1995) 4471–4478.
- [17] L.F. Gibson, J. Fortney, G. Magro, S.G. Ericson, J.P. Lynch, K.S. Landreth, Regulation of BAX and BCL-2 expression in breast cancer cells by chemotherapy, *Breast Canc. Res. Treat.* 55 (1999) 107–117.
- [18] K. Suzuki, T. Kazui, M. Yoshida, T. Uno, T. Kobayashi, T. Kimura, T. Yoshida, H. Sugimura, Drug-induced apoptosis and p53, BCL-2 and BAX expression in breast cancer tissues in vivo and in fibroblast cells in vitro, *Jpn. J. Clin. Oncol.* 29 (1999) 323–331.
- [19] F.H. Sarkar, K.M. Rahman, Y. Li, Bax translocation to mitochondria is an important event in inducing apoptotic cell death by indole-3-carbinol (I3C) treatment of breast cancer cells, *J. Nutr.* 133 (2003) 2434s–2439s.
- [20] K.M. Rahman, O. Aranha, A. Glazyrin, S.R. Chinni, F.H. Sarkar, Translocation of Bax to mitochondria induces apoptotic cell death in indole-3-carbinol (I3C) treated breast cancer cells, *Oncogene* 19 (2000) 5764–5771.
- [21] W. Yu, B.G. Sanders, K. Kline, RRR-alpha-tocopherol succinate-induced apoptosis of human breast cancer cells involves Bax translocation to mitochondria, *Canc. Res.* 63 (2003) 2483–2491.
- [22] D.E. Reyna, T.P. Garner, A. Lopez, F. Kopp, G.S. Choudhary, A. Sridharan, S.R. Narayanagari, K. Mitchell, B. Dong, B.A. Bartholdy, L.D. Walensky, A. Verma, U. Steidl, E. Gavathiotis, Direct activation of BAX by BTA1 overcomes apoptosis resistance in acute myeloid leukemia, *Canc. Cell* 32 (2017) 490–505, e410.
- [23] M. Xin, R. Li, M. Xie, D. Park, T.K. Owonikoko, G.L. Sica, P.E. Corsino, J. Zhou, C. Ding, M.A. White, A.T. Magis, S.S. Ramalingam, W.J. Curran, F.R. Khuri, X. Deng, Small-molecule Bax agonists for cancer therapy, *Nat. Commun.* 5 (2014) 4935.
- [24] G. Liu, T. Yin, H. Kim, C. Ding, Z. Yu, H. Wang, H. Chen, R. Yan, E.A. Wold, H. Zou, X. Liu, Y. Ding, Q. Shen, J. Zhou, Structure-activity relationship studies on Bax activator SMBA1 for the treatment of ER-positive and triple-negative breast cancer, *Eur. J. Med. Chem.* 178 (2019) 589–605.
- [25] K. Nepali, H.-Y. Lee, J.-P. Liou, Nitro-group-containing drugs, *J. Med. Chem.* 62 (2019) 2851–2893.
- [26] C. Limban, D.C. Nuță, C. Chiriță, S. Negreș, A.L. Arsene, M. Goumenou, S.P. Karakitsios, A.M. Tsatsakis, D.A. Sarigiannis, The use of structural alerts to avoid the toxicity of pharmaceuticals, *Toxicol. Rep.* 5 (2018) 943–953.
- [27] N. Miyaura, A. Suzuki, Palladium-catalyzed cross-coupling reactions of organoboron compounds, *Chem. Rev.* 95 (1995) 2457–2483.
- [28] S. Xu, R. Chen, Z. Fu, Q. Zhou, Y. Zhang, J. Wang, Palladium-catalyzed formal [4 + 1] annulation via metal carbene migratory insertion and C(sp²)-H bond functionalization, *ACS Catal.* 7 (2017) 1993–1997.
- [29] K. Kobayashi, Y. Himeji, S. Fukamachi, M. Tanmatsu, O. Morikawa, H. Konishi, Synthesis of 9-arylamino- and (Z)-9-arylimino-9H-pyrrolo[1,2-a]indoles by reactions of 2-(pyrrol-1-yl)benzaldehydes with aryl amines, *Tetrahedron* 63 (2007) 4356–4359.
- [30] F. Grande, F. Aiello, O.D. Grazia, A. Brizzi, A. Garofalo, N. Neamati, Synthesis and antitumor activities of a series of novel quinoxalinhydrazides, *Bioorg. Med. Chem.* 15 (2007) 288–294.
- [31] J. Gui, C.-M. Pan, Y. Jin, T. Qin, J.C. Lo, B.J. Lee, S.H. Spengel, M.E. Mertzman, W.J. Pitts, T.E. La Cruz, M.A. Schmidt, N. Darvatkar, S.R. Natarajan, P.S. Baran, Practical olefin hydroamination with nitroarenes, *Science* 348 (2015) 886–891.
- [32] S. Mikami, S. Sasaki, Y. Asano, O. Ujikawa, S. Fukumoto, K. Nakashima, H. Oki, N. Kamiguchi, H. Imada, H. Iwashita, T. Taniguchi, Discovery of an orally bioavailable, brain-penetrating, in vivo active phosphodiesterase 2A inhibitor lead series for the treatment of cognitive disorders, *J. Med. Chem.* 60 (2017) 7658–7676.
- [33] N. Boechat, A.S. Carvalho, K. Salomão, S.L. Castro, C.F. Araujo-Lima, F.V. Mello, I. Felzenszwalb, C.A. Aiub, T.R. Conde, H.P. Zamith, R. Skupin, G. Haufe, Studies of genotoxicity and mutagenicity of nitroimidazoles: demystifying this critical relationship with the nitro group, *Mem. Inst. Oswaldo Cruz* 110 (2015) 492–499.
- [34] Y. Li, J. Yao, M. Chang, M. Cuendet, J.L. Bolton, Altered apoptotic response in MCF 10A cells treated with the equine estrogen metabolite, 4-hydroxyequilenin, *Toxicol. Lett.* 154 (2004) 225–233.
- [35] S. Bandarra, A.S. Fernandes, I. Magro, P.S. Guerreiro, M. Pingarilho, M.I. Churchwell, O.M. Gil, I. Batinić-Haberle, S. Gonçalves, J. Rueff, Mechanistic insights into the cytotoxicity and genotoxicity induced by glycidamide in human mammary cells, *Mutagenesis* 28 (2013) 721–729.
- [36] J.G. Valero, L. Sancey, J. Kucharczak, Y. Guillemain, D. Gimenez, J. Prudent, G. Gillet, J. Salgado, J.L. Coll, A. Aouacheria, Bax-derived membrane-active peptides act as potent and direct inducers of apoptosis in cancer cells, *J. Cell Sci.* 124 (2011) 556–564.
- [37] L.D. Walensky, E. Gavathiotis, BAX unleashed: the biochemical transformation of an inactive cytosolic monomer into a toxic mitochondrial pore, *Trends Biochem. Sci.* 36 (2011) 642–652.

- [38] P. Friedl, K. Wolf, Tumour-cell invasion and migration: diversity and escape mechanisms, *Nat. Rev. Canc.* 3 (2003) 362–374.
- [39] W. Li, F. Xu, W. Shuai, H. Sun, H. Yao, C. Ma, S. Xu, H. Yao, Z. Zhu, D.H. Yang, Z.S. Chen, J. Xu, Discovery of novel quinoline-chalcone derivatives as potent antitumor agents with microtubule polymerization inhibitory activity, *J. Med. Chem.* 62 (2019) 993–1013.
- [40] L. Lalier, P.F. Cartron, P. Juin, S. Nedelkina, S. Manon, B. Bechinger, F.M. Vallette, Bax activation and mitochondrial insertion during apoptosis, *Apoptosis* 12 (2007) 887–896.
- [41] G. Liu, E.A. Wold, J. Zhou, Applications of bioorthogonal chemistry in tumor-targeted drug discovery, *Curr. Top. Med. Chem.* 19 (2019) 892–897.